UNIVERSITY **POLITEHNICA** of BUCHAREST

Faculty of Applied Chemistry and Materials Science
Department of Inorganic Chemistry, Physical Chemistry and Electrochemistry
Senate Decision No. 124 from 19.07.2017

PhD THESIS SUMMARY

Spectral and electrochemical studies of several pyrrolopyrimidines

Studii electrochimice și spectrale asupra unor pirolopirimidine

Author: Ing. Marian Laurențiu TATU

PhD COMMISION

President	Prof. Dr.Ing. Teodor VISAN	from	University Politehnica of Bucharest
Supervisor	Prof. Dr.Ing. Eleonora-Mihaela UNGUREANU	from	University Politehnica of Bucharest
Reviewer	Prof. Dr.Chim, Elena DIACU	from	University Politehnica of Bucharest
Reviewer	Prof. Dr.Ing. Farm. Gabriela STANCIU	from	University OVIDIUS Constanta
Reviewer	Prof. Dr.Chim. Lucia MUTIHAC	from	University of Bucharest

BUCHAREST
-2017-

Thesis composition

Acknowledgements

Throughout the duration of the PhD degree I had the honor of being guided by people with exceptional human and pedagogical qualities, and I would like to thank them for the time being.

First of all, I would like to thank the PhD coordinator, Prof. Dr. Ing. Eleonora-Mihaela UNGUREANU, for all the support and understanding she has given to me throughout these years. I would like to thank my teacher for all the professionalism with which he has led me and helped me to reach this moment.

I would like to thank the professors from the guidance commission Prof. Chim. Ioana DEMETRESCU, Prof. emeritus Teodor VIŞAN, and S.L. Dr. Ing. George Octavian Buica for all the help and support they have given me whenever I needed it for the entire duration of the doctoral thesis.

I would like to extend my sincere thanks to the members of the doctoral committee: Prof. Dr. Eng. Teodor VISAN, Prof. Dr. Chim. Lucia MUTIHAC, Prof. Dr. Ing. Farm. Gabriela STANCIU, Prof. Dr. Chim. Elena DIACU for the solicitude with which my work was analyzed.
I would also like to thank the co-workers, Dr. Ing. Emilian GEORGESCU from Oltchim Râmnicu Vâlcea and Dr. Marcel POPA from the "Constantin D. Neniţescu" Organic Chemistry Center of the Romanian Academy for their collaboration on synthesis and NMR and FTIR

analyzes of the new compounds As well I want to thank Conf. Dr. Cristian BOSCORNEA from the Faculty of Applied Chemistry and Materials Science, University Politechnica of Bucharest for the help given for the luminescent analysis of the compounds, as well as for all the support that gave me to the interpretation of the experimental data obtained.

Special thanks I would like to bring to all colleagues in the *Electrochemical Process Laboratory* in organic solvents for all the support that they have given me to reach all the goals I have had to achieve throughout the doctoral stage.

I would like to express my sincere thanks for the financial support received through the research contract "Metal Sensors Based on Azulene Modified Electrodes for Water Quality Control", contract no. 236/2014, coordinated by Prof. Dr. Ing Eleonora-Mihaela UNGUREANU.

In conclusion, but last but not least, I would like to thank my family, who supported me during the preparation and elaboration of the doctoral thesis.

The author

INTRODUCTION

The PhD. thesis entitled ELECTROCHEMICAL AND SPECTRAL STUDIES OF SEVERAL PYROLOPYRIMIDINES is part of the research team of the Laboratory of Electrochemical Processes in Organic Solvents (PESO) of POLITEHNICA University of Bucharest (UPB), the Faculty of Applied Chemistry And Materials Science, Department of Inorganic Chemistry, Chemistry-Physics and Electrochemistry.

The thesis was developed within the Faculty of Applied Chemistry and Material Science of UPB and contains original contributions [1-5] in the field of characterization of advanced materials based on pyrrolopyrimidine derivatives. This thesis is part of the PESO team's concern to investigate new derivatives by advanced spectral and electrochemical methods and opens new research directions in the field of floral materials. The research team's concerns regarding the thesis are related to the researches undertaken at the Research Center OLTCHIM Râmnicu Vâlcea, in the field of which the team headed by CS 1 Dr. Ing. Emilian Georgescu has a pioneering contribution in which the syntheses Pyrrolopyrimidine compounds. Also, the research carried out within this thesis benefited from the support and collaboration with Mr. Dr. Marcel-Mirel Popa from the Organic Chemistry Center of the Romanian Academy C.Nenitescu, together with whom the research was carried out to characterize the pyrolopyrimidine derivatives synthesized by NMR and FTIR. In the PESO spectral and electrochemical studies have been studied so far over 50 pyrrolopyrimidine compounds, with which already a database on the electrochemical reactivity of these compounds has been established. In this thesis, besides the original aspects related to the electrochemical characterization of these compounds, the study of a particularly important property of these compounds, namely the florescence, is approached for the first time. The study of these compounds is important because the florescence of heterocycles is of particular interest due to potential applications, from medical applications [6-8] due to biological properties such as anti-microbial, anti-tuberculous, anti-fungal, anti-cancer activity [9] To high-tech materials, such as light emitting diodes (OLEDs) [10-12]. Due to the remarkable fluorescence properties nitrogen-containing heterocycles - especially pyrroloazins [13-15] or pyrrolodiazines [16-20] - have been used to produce fluorescent chemical sensors [21-22], bioprobes [23] DSSCs) [24-26] or LASER dyes [27].

The pyrolo [1,2-c] pyrimidine derivatives studied (Table 1) are part of the bicyclic heteroaromatic systems formed by two condensed cycles [28], having a 5-membered ring fused to a 6-membered ring with a nitrogen atom On the junction and another atom of nitrogen grafted on the 6-atom cycle. In literature, there is currently no data on fluorescence studies of these compounds, which justifies the interstitial investigation of their luminescent properties. Also,

investigating electrochemical properties has been approached for a small number of compounds in this class in electrochemical studies conducted in the PESO lab team.

Table 1. Structure of investigated pyrolo[1,2-c]pyrimidine compounds

Code	R_1	R_2	R_3	R_4	Published papers
		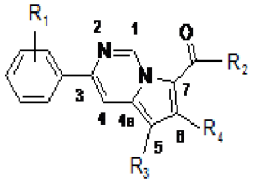			
4a	4-fenil	4-Cl-fenil	COMe	H	[1]
4b	4-fenil	3-NO_2-fenil	COMe	H	[1]
4c	4-fenil	4-F-fenil	CO_2Et	H	[1]
4d	4-fenil	4-Br-fenil	CO_2Et	H	[1]
4e	4-fenil	4-NO_2-fenil	CO_2Et	H	[1]
4f	4-fenil	3,4-diMeO-fenil	CO_2Et	H	[1]
4g	4-fenil	4-NO_2-fenil	CO_2Me	CO_2Me	[1]
4h	4-fenil	4-bifenil	CO_2Et	CO_2Et	[1]
4i	4-fenil	2-naftil	CO_2Et	CO_2Et	[1]
4j	4-fenil	4-NO_2-fenil	COMe	H	[2]
P311	3,4-diMeO	3-NO_2-fenil	CO_2Et	CO_2Et	[4]
P319	2-MeO	fenil	CO_2Me	CO_2Me	[4]
P335	3-MeO	3-NO_2-fenil	CO_2Et	CO_2Et	[4]
P338	2,4-diMeO	4-Br-fenil	CO_2Me	CO_2Me	[4]
P376	3,4-diMeO	4-F-fenil	CO_2Et	H	[4]
P417	3,4,5-triMeO	fenil	CO_2Me	CO_2Me	-
P543	3,4-diMeO	4-Me-fenil	CO_2Et	H	[4]
P545	3,4-diMeO	2-naftil	CO_2Et	H	[3]
P552	3,4-diMeO	2,4-diMeO-fenil	CO_2Et	H	[3, 4]
P557	2,4-diMeO	2-naftil	CO_2Et	H	[5]
P563	2,4-diMeO	4-Me-fenil	CO_2Et	H	[4, 5]
P565	3-Me	3-NO_2-fenil	CO_2Me	CO_2Me	[4]
P585	3,4-diMeO	2,4-diMeO-fenil	CO_2Me	CO_2Me	[4]

The first research direction is related to the synthesis and characterization by NMR and FTIR of new synthesized compounds belonging to the class of pyrrolopyrimidines. Table 1 contains the structure of the pyrolo[1,2-*c*]pyrimidine derivatives studied as well as the literature references in which some of the original results obtained in the thesis were published.

The second direction of research addressed in the thesis is related to the spectral characterization of the new synthesized compounds belonging to the class of pyrrolopyrimidines. Spectroscopy studies (absorption, florescence) were conducted in various organic solvents (chloroform, methylene chloride, acetonitrile (CH3 CN) and dimethyl sulphoxide (DMSO)).

The third research direction in the thesis is related to the electrochemical characterization of the new synthesized compounds belonging to the class of pyrrolopyrimidines. Electrochemical studies were conducted by the methods voltamerie cyclic voltammetry, differential pulse, and the rotating disk electrode obtained by scanning electorzi pyrrolopyrimidines modified or controlled potential electrolysis in CH 3 CN containing tetrabutylammonium perchlorate.

The first part of the thesis entitled REPORT OF LITERATURE (chapters 1-3) shows the data in the literature regarding the current state of knowledge in the field: derivatives of pyrrolo [1,2-c] pyrimidine, spectral methods used in the study of organic compounds, and A brief

presentation of the main electrochemical methods used in the study of organic compounds used in this thesis.

Chapter 1 entitled "Pyrrolo [1,2-c] pyrimidine derivatives" presents the main properties of this class of compounds as well as the main synthetic methods present in the literature as well as data on the electrochemistry of this class of compounds.

Chapter 2 entitled "Spectral Methods Used in the Study of Organic Compounds" refers to the basic principles of spectral techniques used to determine the luminescent properties of the compounds.

Chapter 3 entitled "Electrochemical Methods used in the study of organic compounds" shows the use of electrochemical methods: cyclic voltammetry (CV), differential pulse voltammetry (DPV), the rotating disk electrode (RDE) and the potential-controlled electrolysis (EPC).

The second part of the thesis titled ORIGINAL RESULTS (chapters 4-8) presents the original contributions of the thesis being divided into 5 chapters.

Chapter 4, entitled "Experimental Part", brings attention to information about used reagents, installations, and how to work.

Chapter 5 entitled "Syntheses of Pirolopyrimidines" refers to the actual synthesis of the studied compounds as well as to the NMR and FTIR analyzes performed to confirm the newly obtained chemical structures.

Chapter 6 entitled "Spectral Studies of Pyrolopyrimidines" refers to the luminescent characterization of the series of investigated compounds.

Chapter 7 entitled "Electrochemical studies of some pyrrolopyrimidines" refers to the electrochemical characterization of some pyrrolopyrimidines.

Chapter 8, entitled "Obtaining modified pyrrolopyrimidine electrodes", presents the results of the experiments for the production of pyrrolopyrimidine-modified electrodes by successive cycles and by potentially controlled electrolysis.

The thesis concludes with a bibliography chapter containing 360 bibliographic references, with a list of published papers and conferences in which disseminated the results of the researches carried out during the PhD thesis and the annexation of the papers published in extenso.

II. ORIGINAL REZULTS

CAPITOL 4. EXPERIMENTAL PART

4.1. REAGENTS

4.1.1. Reagents use for synthesis

4-biphenylpyrimidine, substituted 4-phenylpyrimidines, substituted phenacyl bromides and activated alkynes 3-butyn-2-one, ethyl propiolate, methyl acetylenedicarboxylate and ethyl acetylenedicarboxylate) have benn used to obtain pyrrolo[1,2-c] pyrimidine. The substituted phenacyl bromides, 1,2-epoxybutane and the solvents used in the synthesis (chloroform, methanol and ethyl ether) were obtained from Sigma Aldrich. The 4-phenylpyrimidine derivatives were provided by colleagues at the Oltchim Research Center Ramnicu Valcea. 4-Biphenylpyrimidine was obtained from 4-acetylbiphenyl and trisformylaminomethane according to the method reported in the literature for the synthesis of 4-phenylpyrimidine [348]. The synthesis of 4-biphenylpyrimidine is shown in Chapter. 4.3.1.

4.1.2. Reagents use for spectral studies

The solvents acetonitrile (CH_3CN), chloroform (CH_3Cl), dichloromethane (CH_2Cl_2), dimethylsulfoxide (DMSO) and concentrated sulfuric acid (H_2SO_4) (from Fluka) have been used for spectral studies. Quinine sulphate (Buchler) was used as standard for calculation of the quantum yield, and 1,4-benzoquinone (Sigma) was used as quencher.

4.1.3. Reagents use for electrochemical studies

The pyrrolopyrimidine compounds were synthesized according to the procedure described in Chapter 5. Electrochemical determinations were carried out under argon at 20° C using acetonitrile as solvent and Fluka perchlorate tetrachloride salt (TBAP) analytical purityfrom Fluka. The reference electrode Ag /AgNO3 10 mM in 0.1 M TBAP, CH3 CN was prepared from AgNO3 (Riedel).

4.2. EXPERIMENTAL INSTALLATIONS AND EQUIPMENT

4.2.1. Installations and equipment for the synthesis of pyrrolopyrimidines

The synthesis of 4-biphenylpyrimidine was carried out in a 500 mL round bottom flask placed in a heating nest and equipped with an upward refrigerant connected to a water tube for a weak capillary vacuum and thermometer.

The structures of the compounds obtained were investigated by carbon NMR and hydrogen NMR using a Varian Gemini 300 BB instrument. Elemental analysis was performed with a COSTECH Instruments EAS32 instrument. IR spectra were recorded with a Nicolet Impact 410 spectrometer, and the melting point was determined using a Boëtius microscope.

4.2.2. Installations and equipment for spectral studies

The absorbance spectra of the investigated compounds were recorded using a JASCO V550 spectrophotometer at room temperature. Under the same conditions, fluorescence spectra were recorded but using a JASCO FP 6500 spectrophotometer which reads at an angle of 90^0. The refractive indices of the solutions which were subjected to luminescence determinations were measured with an Abbe refractometer from CETI Belgium.

4.2.3. Installations and equipment for electrochemical studies

Electrochemical determinations of pyrrolo[1,2-c]pyrimidine derivatives were performed with a PGSTAT 12 AUTOLAB potentiostat. The electrochemical cell used was a conventional three electrode cell: a working electrode - vitreous carbon disk (3 mm diameter), a 10 mM Ag / $AgNO_3$ in 0.1 M TBAP reference electrode and a platinum wire counter electrode.

4.3. EXPERIMENTAL TECHNIQUES FOR THE STUDY OF INVESTIGATED COMPOUNDS

4.3.1. Experimental techniques for the synthesis of pyrrolopyrimidines

- Working mode for the synthesis of 4-biphenylpyrimidine

In a 500 mL flask equipped as shown in the head. 4.2.1, 120 mL (3 moles) of formamide and 28.5 mL (0.3 moles) of dimethyl sulphate were introduced. The mixture was heated at 85-90°C under vacuum and maintained at this temperature for two hours. Vacuum was discontinued, capillary removed and 28 g (0.15 mole) of 4-acetylbiphenyl and 0.7 g of p-toluenesulfonic acid were added to the flask. The reaction mixture was slowly warmed to 155-160 ° C and held for eight hours at this temperature. The mixture was cooled, 100 mL of 1 N NaOH solution was added and extracted with chloroform (3 x 250 mL). The combined chloroform extracts were dried over anhydrous Na 2 SO 4, the solvent was removed in vacuo and the product was distilled under vacuum (3-5 mm Hg, 180-190 ° C). 23.6 g (68%) of white-yellow solid with mp = 193-196 ° C were obtained.

4.3.2. Experimental techniques for specral studies

For the luminescence studies, stock solutions of known concentration were prepared. By successive dilutions, the concentrations used were obtained. Absorbance spectra identified peak absorption wavelengths, which were later used in fluorescence studies.The emission curves were recorded at the wavelength corresponding to the maximum absorption lengths. Calculation of quantum yield was made against a freely chosen standard whose quantum yield is known. - a

solution of quinine sulphate 10-6 mol / L in 0.5 M H_2SO_4. The fluorescence extinction was done in the presence of the 1,4-benzoquinone extinguisher which was gradually added from a stock solution to the solution of the compound whose fluorescence was tested (10-6 M), the emission spectrum being recorded after each addition. The fluorescence spectra processing for calculating the fluorescence parameters are described in more detail below in Chapter 6 of the thesis.

4.3.3. Experimental techniques for electrochemical studies

The electrochemical experiments used to characterize the new compounds were: cyclic voltammetry (CV) at a scanning rate of 0.1 V/s or at different scanning rate (0.2, 0.3, 0.5, 1 V/s) in the case of the study of the influence of this parameter, differential pulse voltammetry (DPV) with a scanning rate of 0.01 V/s, voltammetry on a rotating disc electrode (RDE) with a scanning rate of 0.01 V/s at electrode rotation speeds 500 - 2000 rpm.

In the case of electrochemical studies, solutions of the studied derivatives (0.75 mM) were prepared by dissolving them in the support electrolyte. After the CV, DPV and RDE curves were detected by dilution, the following concentration (0.5 mM) was performed for the influence of the scanning speed on the scaling effect and for which modified electrodes (by cycling Successive to different potentials and by EPC). The work electrode was cleaned by grinding on a diamond paste (0.25 μm) before each recording.

CHAPTER 5
SYNTHESIS OF PIROLOPIRIMIDINE

5.1. SYNTHESIS OF 3-BIPHENIL PYRROLO[1,2-*c*]PYRIMIDINES DERIVATIVES

New derivatives of 3-biphenylpyrrolo[1,2-*c*]pyrimidine (Table 5.1) were synthesized according to methods reported in the literature [59-60]. The method chosen for the synthesis was "one-pot tree components" which aims to obtain in a single step, in the same balloon, new complex compounds starting from simple raw materials, these being found as constituents in the structure of the new compounds [59-60]. This method involves the 1,3-dipolar cycloaddition reaction of 4-biphenylpyrimidine and an electron deficient leucine in 1,2-epoxybutane at reflux. The advantage of this reaction (Scheme 5.1) is the direct formation of 3-biphenylpyrrolo [1,2-c] pyrimidine, without inactivation and good yields [1,2,59,60,39].

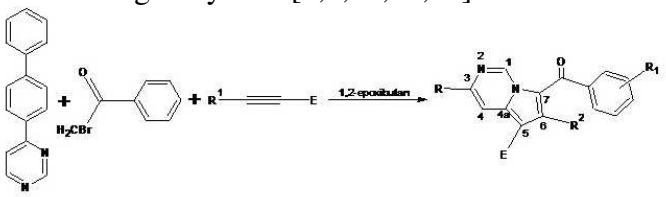

Scheme 5.1. Synthesis of 3-biphenylpyrrolo[1,2-*c*]pyrimidine derivatives (R = biphenyl)

Scheme 5.2 presents the mechanism of reaction to obtain new compounds. This involves the formation of a highly reactive alkoxide due to the attack of the pyrimidinium bromide bromide ion (5) on the 1,2-epoxybutane ring. The alkoxide extracts a proton from pyrimidinium bromide (5) to give pyrimidinium-N-ylid (6) which further reacts as a mesomeric 1,3 dipole. In the last step, a 1,3-dipolar cycloaddition reaction occurs between pyrimidinium-N-ylid 6 and activated alkyne which leads to the formation of the cycloaduct (8) which, by oxidation under the reaction conditions, results in the final aromatic compound [1, 2, 350, 351].

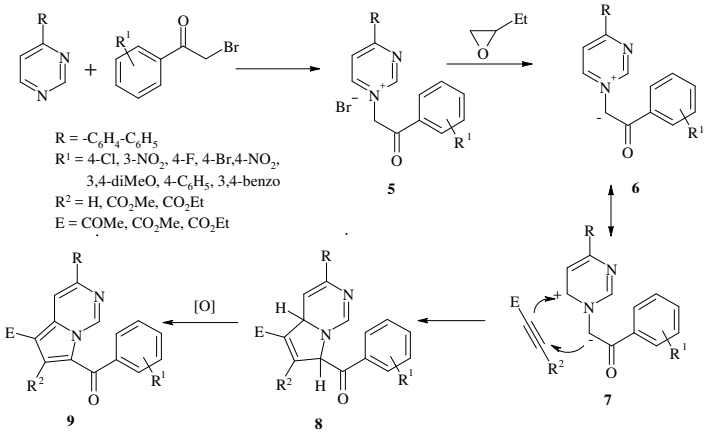

Scheme 5.2. The mechanism for the synthesis of 3-biphenylpyrrolo[1,2-c] yrimidine derivatives

Table 5.1. Structures, melting points and synthesis yield for new pyrrolo[1,2-c] yrimidine

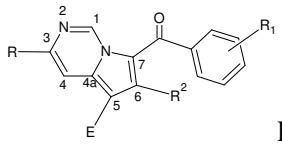

R = bifenil

Compound	R^1	R^2	E	Mp (^{o}C)	Yield (%)
4a	4-Cl	H	COMe	234-235	53
4b	3-NO_2	H	COMe	286-288	49
4c	4-F	H	CO_2Et	222-224	58
4d	4-Br	H	CO_2Et	234-235	53
4e	4-NO_2	H	CO_2Et	267-269	47
4f	3,4-diMeO	H	CO_2Et	216-218	55
4g	4-NO_2	CO_2Me	CO_2Me	286-288	62
4h	4-C_6H_5	CO_2Et	CO_2Et	216-218	51
4i	3,4-benzo	CO_2Et	CO_2Et	215-217	44
4j	4-NO_2	H	COMe	295-297	65

The structure of the new obtained compounds was determined by FTIR spectroscopy, NMR and elemental analysis. All the experimental data are consistent with the proposed structures [1, 2, 351].

3-(4-Biphenylyl)-5-acetyl-7-(4-chlorobenzoyl)pyrrolo[1,2-c]pyrimidine (4a). Yellow crystals. FT-IR (ATR, cm-1):3096, 1667, 1610, 1513, 1467, 1328, 1219, 1194;1H-NMR (CDCl3, 400 MHz, δ): 2.56 (s, 3H, CH3); 7.38-7.41 (m, 2H, 2H-Ph); 7.46-7.51 (m, 1H, 1H-Ph); 7.70 (s, 1H, H-6); 7.67-7.69 (m, 2H, 2H-Ph); 7.55, 7.82 (2d, J = 8.4 Hz, H-2", H-3", H-5", H-6"); 7.77 (d, J = 8.4 Hz, 2H, H-2', H-6'); 8.30 (d, J = 8.4 Hz, 2H, H-2', H-6'); 8.93 (d, J = 1.1 Hz, 1H, H-4); 10.62 (d, J = 1.1 Hz, 1H, H-1). 13C-NMR (CDCl3, 100 MHz, δ): 28.1 (Me); 109.3 (C-4); 115.4 (C-5); 127.7, 127.9, 128.9, 129.5, 130.3, (C-2", C-3", C-5", C-6", 5C-Ph); 121.9, 135.2, 137.4, 138.6, 140.2, 140.8, 143.1, 151.2 (C-7, C-4a, C-3, C-1', C-4', C-1", C-4" Cq-Ph); 127.1, 127.5 (C-2', C-3', C-4', C-6'); 129.0 (C-6); 140.7(C-1); 183.9 (COAr), 193.01 (COMe); Anal. calcd. C28H19ClN2O2 (450.91): C 74.58; H 4.25; N 6.21. Found: C 74.64, H 4.29, N 6.17.

3-(4-Biphenylyl)-5-acetyl-7-(3-nitrobenzoyl)pyrrolo[1,2-c]pyrimidine (4b). Yellow-mustard crystals. FT-IR (KBr, cm-1): 3085, 1664, 1617, 1600, 1530, 1515, 1481, 1416, 1350, 1329, 1219, 1196, 1110, 1006. 1H-NMR (CDCl3+TFA, 300 MHz, δ): 2.76 (s, 3H, CH3); 7.44-7.54 (m, 4H, H-5", 3H-Ph); 7.66-7.70 (m, 2H, 2H-Ph); 7.89 (s, 1H, H-6); 7.86-7.90 (m, 2H, H-3', H-5'); 8.05 (d, J = 8.4 Hz, 2H, H-2', H-6'); 8.23-8.25 (m, 1H, H-4"); 8.57-8.60 (m, 1H, H-6");

8.72 (t, J = 1.9 Hz, 1H, H-2”); 8.06 (d, J = 8.4, 2H, H-2’, H-6’); 9.01 (d, J = 1.1 Hz, 1H, H-4); 11.25 (d, J = 1.1 Hz, 1H, H-1). 13C-NMR (CDCl3+TFA, 75 MHz, δ): 27.5 (Me); 112.0 (C-4); 116.4 (C-5); 123.9 (C-2”) 127.3, 127.8, 128.1, 128.5, 128.6, 129.1, 132.7, 134.7 (C-2’, C-3’, C-5’, C-6’, C-4”, C-5”, C-6”, 5C-Ph); 123.3, 138.6, 139.3, 141.0, 143.5, 145.5, 148.4 (C-7, C-4a, C-3, C-1’, C-4’, C-1”, C-3", Cq-Ph); 130.7 (C-6); 141.0 (C-1); 184.9 (COAr), 197.3 (COMe); Anal. calcd. C28H19N3O4 (461.47): C 72.88; H 4.15; N 9.10. Found: C 72.93, H 4.18, N 9.03.

Ethyl 3-(4-biphenylyl)-7-(4-fluorobenzoyl)pyrrolo[1,2-c]pyrimidine-5-carboxylate (4c) Yellow crystals. FT-IR (KBr, cm-1): 3068, 2976, 1700, 1616, 1523, 1470, 1416, 1330, 1230, 1199, 1154, 1085, 1052. 1H-NMR (CDCl3, 300 MHz, δ): 1.45 (t, J = 7.1 Hz, 3H, CH3); 4.43 (q, J = 7.1 Hz, 2H, CH2); 7.21(t, J = 8.6 Hz, 2H, H-3”, H-5”); 7.35-7.49 (m, 3H, 3H-Ph); 7.63-7.70 (m, 2H, 2H-Ph); 7.72 (d, J = 8.5 Hz, 2H, H-3’, H-5’); 7.75 (s, 1H, H-6); 7.86-7.88 (m, 2H, H-2”, H-6”); 8.21 (d, J = 8.5 Hz, 2H, H-2’, H-6’); 8.62 (d, J = 1.1 Hz, 1H, H-4); 10.54 (d, J = 1.1 Hz, 1H, H-1); 13C-NMR (CDCl3, 75 MHz, δ): 14.7 (Me); 60.8 (CH2); 107.2 (C-5); 108.5 (C-4); 115.9 (J = 21.8 Hz, C-3”, C-5”); 122.2, 135.3, 135.5 140.3, 140.9, 142.9, 149.6 (C-7, C-4a, C-3, C-1’, C-4’, C-1”, Cq-Ph); 127.2, 129.0 (C-2’, C-3’, C-5’, C-6’); 129.8 (C-6); 127.4, 127.7, 128.0 (5C-Ph); 131.5 (J = 8.9 Hz, C-2”, C-6”); 140.8 (C-1); 165.2 (J = 263.4 Hz, C-4”); 163.7 (CO); 183.8 (COAr); Anal. calcd. C29H21FN2O3 (464.50): C 74.99; H 4.56; N 6.03. Found: C 75.05, H 4.52, N 5.99.

Ethyl 3-(4-biphenylyl)-7-(4-bromobenzoyl)pyrrolo[1,2-c]pyrimidine-5-carboxylate (4d). Yellow crystals. FT-IR (KBr, cm-1): 3108, 3054, 2985, 1698, 1620, 1600, 1521, 1472, 1430, 1351, 1327, 1300, 1253, 1202, 1087, 1048; 1H-NMR (CDCl3+TFA, 300 MHz, δ): 1.49 (t, J = 7.1 Hz, 3H, CH3); 4.50 (q, J = 7.1 Hz, 2H, CH2); 7.41-7.53 (m, 3H, 3H-Ph); 7.66-7.69 (m, 2H, 2H-Ph); 7.73-7.74 (m, 4H, H-2”, H-3”, H-5”, H-6”); 7.83 (d, J = 8.6 Hz, 2H, H-2’, H-6’); 8.03 (d, J = 8.6 Hz, 2H, H-2’, H-6’); 8.04 (s, 1H, H-6); 8.69 (d, J = 1.1 Hz, 1H, H-4); 11.08 (d, J = 1.1 Hz, 1H, H-1); Anal. calcd. C29H21BrN2O3 (525.39): C 66.29; H 4.03; N 5.33. Found: C 66.36, H 4.10, N 5.28.

Ethyl 3-(4-biphenylyl)-7-(4-nitrobenzoyl)pyrrolo[1,2-c]pyrimidine-5-carboxylate (4e). Orange crystals. FT-IR (KBr, cm-1): 2983, 1701, 1617, 1591, 1523, 1471, 1415, 1347, 1327, 1254, 1203, 1089, 1053. 1H-NMR (CDCl3, 300 MHz, δ): 1.45 (t, J = 7.1 Hz, 3H, CH3); 4.44 (q, J = 7.1 Hz, 2H, CH2); 7.40-7.52 (m, 3H, 3H-Ph); 7.67-7.70 (m,2H, 2H-Ph); 7.77 (d, J = 8.4 Hz, 2H, H-3’, H-5’); 7.78 (s, 1H, H-6); 8.00 (d, J = 8.8 Hz, 2H, H-3”, H-5”); 8.27 (d, J = 8.4 Hz, 2H, H-2’, H-6’); 8.41 (d, J = 8.8 Hz, 2H, H-2”, H-6”); 8.71 (d, J = 1.1 Hz, 1H, H-4); 10.64 (d, J = 1.1 Hz, 1H, H-1); 13C-NMR (CDCl3, 75 MHz, δ): 27.7 (Me); 60.6 (CH2); 107.7 (C-5); 108.4 (C-4); 123.8, (C-3”, C-5”); 121.5, 135.0, 140.0, 141.4, 143.0, 144.2, 149,6, 150.3 (C-7, C-4a, C-3, C-1’, C-4’, C-1”, C-4”, Cq-Ph); 130.2 (C-6); 127.0, 127.3, 127.6, 127.8, 128.9, 129.7 (C-2’, C-3’, C-5’, C-6’, C-2”, C-6”,5C-Ph); 140.6 (C-1); 163.2 (CO); 184.9 (COAr); Anal. calcd. C29H21N3O5 (491.49): C 70.87; H 4.31; N 8.55. Found: C 70.82, H 4.28, N 8.61.

Ethyl 3-(4-biphenylyl)-7-(3,4-dimethoxybenzoyl)pyrrolo[1,2-c]pyrimidine-5-carboxylate (4f). Yellow crystals. FT-IR (KBr, cm-1): 2935, 2839, 1706, 1619, 1602, 1516, 1475, 1416, 1328, 1266, 1198, 1172, 1140, 1091, 1050, 1024. 1H-NMR (CDCl3, 300 MHz, δ): 1.38 (t, J = 7.1 Hz, 3H, CH3); 3.90 (s, 3H, OMe); 3.91 (s, 3H, OMe); 4.36 (q, J = 7.1 Hz, 2H, CH2); 6.90 (d, J = 8.4 Hz, 1H, H-5”); 7.30-7.48 (m, 5H, H-2”, H-6”, 3H-Ph); 7.58-7.60 (m, 2H, 2H-Ph); 7.68 (d, J = 8.5 Hz, 2H, H-3’, H-5’); 7.78 (s, 1H, H-6); 8.17 (d, J = 8.5 Hz, 2H, H-2’, H-6’); 8.57 (d, J = 1.1 Hz, 1H, H-4); 10.46 (d, J = 1.1 Hz, 1H, H-1); 13C-NMR (CDCl3, 75 MHz, δ): 14.6 (Me); 56.1 (2OMe); 60.5 (CH2); 106.8 (C-5); 108.4 (C-4); 110.2, 111.6, 123.6 (C-2”, C-5”, C-6”); 122.4, 131.6, 135.5 140.3, 140.6, 142.7, 149.2 (C-7, C-4a, C-3, C-1’, C-4’, C-1”, Cq-Ph); 127.2, 127.3 (C-2’, C-3’, C-5’, C-6’); 129.3 (C-6); 127.1, 127.6, 128.9 (5C-Ph); 140.8 (C-1); 149.3,

152.8 (C-3", C-4"); 163.7 (CO); 184.0 (COAr); Anal. calcd. C31H26N2O5 (506.55): C 73.50; H 5.17; N 5.53. Found: C 73.61, H 5.22, N 5.49.

Dimethyl 3-(4-biphenylyl)-7-(4-nitrobenzoyl)pyrrolo[1,2-c]pyrimidine-5,6-dicarboxylate (4g). Orange crystals. FT-IR (KBr, cm-1): 3072, 2957, 1739, 1697, 1619, 1601, 1529, 1508, 1497, 1445, 1387, 1350, 1337, 1251, 1205, 1176, 1106. 1H-NMR (CDCl3+TFA, 300 MHz, δ): 3.47 (s, 3H, CH3); 4.03 (s, 3H, CH3); 7.43-7.54 (m, 3H, 3H-Ph); 7.55-7.66 (m, 2H, 2H-Ph); 7.84-8.02 (m, 6H, H-2', H-3', H-5', H-6', H-2", H-6"); 8.38 (d, J = 8.5 Hz, 1H, H-3", H-5"); 8.69 (d, J = 1.5 Hz, 1H, H-4); 10.96 (d, J = 1.5 Hz, 1H, H-1); 13C-NMR (CDCl3+TFA, 75 MHz, δ): 53.4, 53.9 (2CH3); 107.0 (C-5); 111.4 (C-4); 121.0, 131.2, 135.3, 139.4, 142.6, 143.6, 145.1, 148.0, 150.4 (C-6, C-7, C-4a, C-3, C-1', C-4', C-1", C-4", Cq-Ph); 127.3, 128.0, 128.5, 128.6, 129.2 (C-2', C-3', C-5', C-6', 5C-Ph); 123.9, 129.9 (C-2", C-3", C-5", C-6"); 139.4 (C-1); 163.3, 165.0 (2CO); 185.0 (COAr); Anal. calcd. C30H21N3O7 (535.50): C 67.29; H 3.95; N 7.85. Found: C 67.35, H 3.99, N 7.81.

Diethyl 3-(4-biphenylyl)-7-(4-phenylbenzoyl)pyrrolo[1,2-c]pyrimidine-5,6-dicarboxylate (4h). Yellow crystals. FT-IR (KBr, cm-1): 2972, 1734, 1700, 1611, 1605, 1490, 1431, 1395, 1371, 1333, 1243, 1196, 1103. 1H-NMR (CDCl3, 300 MHz, δ): 1.04 (t, J = 7.1 Hz, 3H, CH3); 1.38 (t, J = 7.1 Hz, 3H, CH3); 3.74 (q, J = 7.1 Hz, 2H, CH2); 4.38 (q, J = 7.1 Hz, 2H, 2CH2); 7.38-7.51 (m, 6H, 6H-Ph); 7.62-7.84 (m, 10H, H-2', H-6', H-2", H-3", H-5", H-6" 4H-Ph); 8.24 (d, J = 8.4 Hz, 2H, H-3', H-5'); 8.67 (d, J = 1.5 Hz, 1H, H-4); 10.29 (d, J = 1.5 Hz, 1H, H-1); 13C-NMR (CDCl3, 75 MHz, δ): 13.6, 14.3 (2Me); 60.8, 62.0 (2CH2); 104.9 (C-5); 108.5 (C-4); 120.4, 132.8, 135.2, 137.6, 139.6, 139.8, 140.9, 143.0, 145.3, 149.6 (C-6, C-7, C-4a, C-3, C-1', C-4', C-1", C-4", 2Cq-Ph); 127.3, 127.4, 129.1, 129.5 (C-2', C-3', C-5', C-6', C-2", C-3", C-5", C-6"); 126.9, 127.1, 127.7, 127.9, 128.3, 128.9 (10C-Ph); 140.4 (C-1); 162.7, 164.2 (2CO); 186.0 (COAr); Anal. calcd. C38H30N2O5 (594.65): C 76.75; H 5.08; N 4.71. Found: C 76.80, H 5.11, N 4.66.

Diethyl 3-(4-biphenylyl)-7-(2-naphthoyl)pyrrolo[1,2-c]pyrimidine-5,6-dicarboxylate (4i).Yellow crystals. FT-IR (KBr, cm-1): 2979, 1739, 1697, 1619, 1508, 1489, 1431, 1383, 1334, 1245, 1200, 1183, 1128, 1093. 1H-NMR (CDCl3, 300 MHz, δ): 0.9 (t, J = 7.1 Hz, 3H, CH3); 1.39 (t, J = 7.1 Hz, 3H, CH3); 3.40 (q, J = 7.1 Hz, 2H, CH2); 4.41 (q, J = 7.1 Hz, 2H, CH2); 7.38-7.56 (m, 3H, 3H-Ph); 7.57-7.77 (m, 7H, H-2', H-6', 2H-Ph, 4H-Naphthoyl); 7.90-7.98 (m, 2H, 2H-Naphthoyl); 8.26 (br s, 1H, 1H-Naphthoyl); 8.27 (d, J = 8.4 Hz, 2H, H-3', H-5'); 8.72 (d, J = 1.5 Hz, 1H, H-4); 10.35 (d, J = 1.5 Hz, 1H, H-1); 13C-NMR (CDCl3, 75 MHz, δ): 13.1, 14.1 (2Me); 60.6, 60.7 (2CH2); 104.8 (C-1); 108.3 (C-8); 120.4, 130.3, 131.7, 132.8, 135.0, 135.8, 139.5, 140.1, 142.2, 149.2 (C-6, C-7, C-4a, C-3, C-1', C-4', 1Cq-Ph, 3Cq-Naphthoyl); 127.2, 129.1 (C-2', C-3', C-5', C-6'); 124.4, 126.8, 126.9, 127.4, 127.5, 127.7, 128.2, 128.4, 128.7, 130.3 (5C-Ph, 7C-Naphthoyl); 140.2 (C-1); 162.5, 164.0 (2CO); 186.0 (COAr); Anal. calcd. C36H28N2O5 (568.62): C 76.04; H 4.96; N 4.93. Found: C 75.99, H 4.92, N 4.89.

3-(4-*biphenyly)-5-acetyl--(4-nitrobenzoyl)pyrrolo[1,2-c]pyrimidine (4j).* Cristale portocalii. FT-IR (KBr, cm^{-1}): 3094, 3066, 1654, 1623, 1599, 1515, 1485, 1472, 1419, 1346, 1332, 1222, 1194, 1090.^{1}H-NMR ($CDCl_3$+TFA, 300 MHz, δ): 2.76 (s, 3H, CH_3); 7.45-7.54 (m,3H, 3H-Ph); 7.67-7.70 (m,2H, 2H-Ph); 7.87-8.09 (m , 7H, H-2, H-2', H-3', H-5', H-6', H-2", H-6"); 8.47 (d, *J* = 8.8 Hz, 2H, H-3", H-5"); 9.04 (d, *J* = 1.1 Hz, 1H, H-8); 11.32 (d, *J* = 1.1 Hz, 1H, H-5).^{13}C-NMR ($CDCl_3$+TFA, 75 MHz, δ): 27.7 (Me); 112.5 (C-8); 116.7 (C-1); 124.6, 127.3, 128.1, 128.7, 128.8, 130.1, 133.6 (C-2", C-4", C-5", C-6", C-2', C-3', C-5', C-6', 5C-Ph); 123.8, 133.6, 139.3, 142.3, 143.9, 145.9, 150.5, 153.2 (C-3, C-8a, C-7, C-1', C-4', C-1", C-4", Cq-Ph); 130.5 (C-2); 140.7 (C-5); 184.6 (COAr), 197.9 (COMe); Anal.calcd. $C_{28}H_{19}N_3O_4$ (461.47): C 72.88; H 4.15; N 9.10. Found: C 72.83, H 4.20, N 9.13.

5.2. SYNTHESIS OF 3-PHENIL PYRROLO[1,2-*c*]PYRIMIDINES DERIVATIVES

Pyrrolo[1,2-c]pyrimidines 3-15 (Table 5.2) were synthesized by the 1,3-dipolar cycloaddition reaction of pyrimidinium bromide with a dipolarophilic alkylate in 1,2-epoxybutane, used as acceptor and solvent (Scheme 5.3), as described above [1, 2, 350, 351].

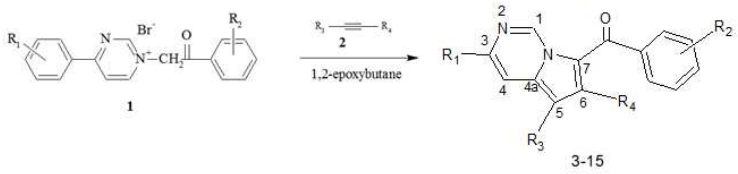

Scheme 5.3. Synthesis of 3-phenylpyrrolo[1,2-c]pyrimidine derivatives

Table 5.2. Structure of the investigated 3-phenylpyrolo[1,2-*c*]pyrimidine derivatives

Compound	Cod	R^1	R^2	R^3	R^4	m.p. (°C)
			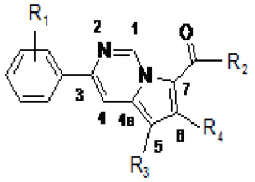			
3	P319	2-MeO	fenil	CO_2Me	CO_2Me	180-182
4	P335	3-MeO	3-NO_2-fenil	CO_2Et	CO_2Et	209-211
5	P338	2,4-diMeO	4-Br-fenil	CO_2Me	CO_2Me	197-199
6	P563	2,4-diMeO	4-Me-fenil	CO_2Et	H	106-108
7	P376	3,4-diMeO	4-F	CO_2Et	H	223-225
8	P543	3,4-diMeO	4-Me-fenil	CO_2Et	H	221-223
9	P311	3,4-diMeO	3-NO_2-fenil	CO_2Et	CO_2Et	166-168
10	P552	3,4-diMeO	2,4-diMeO-fenil	CO_2Et	H	237-239
11	P585	3,4-diMeO	2,4-diMeO-fenil	CO_2Me	CO_2Me	163-164 [60]
12	P565	3-Me	3-NO_2-fenil	CO_2Me	CO_2Me	195-199 [60]
13	**P417**	3,4,5-triMeO	fenil	CO_2Me	CO_2Me	193-195[60]
14	**P545**	3,4-diMeO	2-naftil	CO_2Et	H	238-241
15	**P557**	2,4-diMeO	2-naftil	CO_2Et	H	230-231

Dimethyl 3-(2-methoxyphenyl)-7-benzoyl-pyrrolo[1,2-c]pyrimidine-5,6-dicarboxylate (P319): yellow crystals; 0.43 g (39%). IR (cm-1): 2945, 1746, 1697, 1626, 1518, 1490, 1448, 1382, 1344, 1303, 1265, 1202, 1167, 1108.1H NMR (300 MHz, CDCl3) δ: 3.34, 3.91, 3.99 (3s, 6H, 3MeO); 7.06 (dd, 1H, J = 8.3, 1.1 Hz, H-3'); 7.13 (td, 1H, J = 7.8, 1.1 Hz, H-5');7.41-7.61 (2m, 4H, H-4', H-3", H-4", H-5"); 7.71-7.74 (m, 2H, H-2", H-6"); 8.18 (dd, 1H, J = 7.8, 1.8 Hz, H-6'); 8.95 (d, 1H, J = 1.5 Hz, H-4); 10.30 (d, 1H, J = 1.5 Hz, H-1). 13C NMR (75 MHz, CDCl3) δ: 51.7, 52.3, 55.6 (3MeO); 104.7 (C-5); 111.5 (C-3'); 113.5 (C-4); 120.2 (C-7); 121.1, 130.9, 131.0 (C-4', C-5', C-6'); 128.1, 128.6, 132.1 (C-2", C-3", C-4", C-5", C-6"); 125.5, 132.8, 138.9, 139.0 (C-4a, C-6, C-1', C-1"); 139.7 (C-1); 147.9 (C-3); 157.9 (C-2'); 162.9, 164.5 (2COO); 186.3 (COAr). Anal. Calcd. for C25H20N2O6 (444.44): C 67.56, H 4.54, N 6.30. Found C 67.63, H 4.61, N 6.22.

Diethyl 3-(3-methoxyphenyl)-7-(3-nitrobenzoyl)pyrrolo[1,2-c]pyrimidine-5,6-carboxylate (P335): yellow crystals; 0.66 g (51%). IR (cm-1): 2986, 1732, 1707, 1619, 1530, 1493, 1439, 1340, 1224, 1197, 1118.1H NMR (300 MHz, CDCl3) δ: 1.09, 1.38 (2t, 6H, J = 7.1 Hz, 2CH3); 3.92 (s, 3H, MeO); 3.75, 4.40 (2q, 4H, J = 7.1 Hz, 2CH2); 7.02-7.06 (m, 1H, H-4'); 7.44 (t, 1H, J = 7.8 Hz, H-5'); 7.66-7.76 (m, 3H, H-2', H-6', H-5");8.04-8.07 (m, 1H, H-6"); 8.42-8.46 (m, 1H, H-4"); 8.57 (t, 1H, J = 1.8 Hz, H-2"); 8.65 (d, 1H, J = 1.5 Hz, H-4); 10.37 (d, 1H, J = 1.5 Hz, H-1). Anal. Calcd. for C27H23N3O8 (517.49): C 62.66, H 4.48, N 8.12. Found C 62.74, H 4.52, N 8.03.

Dimethyl 3-(2,4-dimethoxyphenyl)-7-(4-bromobenzoyl)pyrrolo[1,2-c]pyrimidine-5,6-dicarboxylate (P338): yellow crystals;0.57 g (41%). IR (cm-1): 2945, 1739, 1704, 1605, 1502, 1446, 1386, 1292, 1261, 1201, 1177, 1106.1H NMR (300 MHz, CDCl3) δ: 3.41, 3.89, 3.91, 3.98 (2s, 6H, 2MeO); 6.58 (d, 1H, J = 2.5 Hz, H-3'); 6.66 (dd, 1H, J = 8.2, 2.5 Hz, H-5');7.57 (d, 2H, J = 8.8 Hz, H-2", H-6"); 7.62 (d, 2H, J = 8.8 Hz, H-3", H-5"); 8.24 (d, 1H, J = 8.8 Hz, H-6'); 8.93 (d, 1H, J = 1.5 Hz, H-4); 10.25 (d, 1H, J = 1.5 Hz, H-1). Anal. Calcd. for C26H21BrN2O7 (553.36): C 56.43, H 3.82, N 5.06. Found C 56.38, H 3.76, N 5.11.

Ethyl 3-(2,4-dimethoxyphenyl)-7-(4-methylbenzoyl)pyrrolo[1,2-c]pyrimidine-5-carboxylate (P563): yellow crystals;0.53 g (48 %).IR (cm-1): 2985, 1686, 1612, 1572, 1523, 1472, 1408, 1349, 1327, 1299, 1257, 1206, 1087.1H NMR (300 MHz, CDCl3) δ:1.44 (t, 3H, J = 7.1 Hz, CH3); 2.46 (s, 3H, CH3); 3.87, 3.97 (2s, 6H, 2MeO); 4.40 (q, 2H, J = 7.1 Hz, CH2); 6.57 (d, 1H, J = 2.5 Hz, H-3'); 6.64 (dd, 1H, J = 8.2, 2.5 Hz, H-5'); 7.33 (d, 2H, J = 8.8 Hz, H-2", H-6"); 7.76 (d, 2H, J = 8.2 Hz, H-3", H-5"); 7.83 (s, 1H, H-6); 8.22 (d, 1H, J = 8.8 Hz, H-6'); 8.90 (d, 1H, J = 1.5 Hz, H-4); 10.52 (d, 1H, J = 1.5 Hz, H-1). 13C NMR (75 MHz, CDCl3) δ: 14.7 (CH3); 21.7 (CH3); 55.6, 55.7 (2MeO); 60.4 (CH2); 99.0 (C-3'); 105.3 (C-5'); 106.6 (C-5); 112.2 (C-4); 118.8 (C-1'); 122.2 (C-7); 129.5 (C-6, C-3", C-5"); 130.1 (C-2", C-6"); 132.3 (C-6'); 140.3 (C-1); 136.6, 140.6, 142.6, (C-4a, C-1", C-4"); 147.5 (C-3);159.4, 162.2 (C-2', C-4'); 163.9 (COO);185.0 (COAr). Anal. Calcd. for C26H24N2O5 (444,48): C 70.26, H 5.44, N 6.30. Found C 70.37, H 5.53, N 6.22.

Ethyl 3-(3,4-dimethoxylphenyl)-7-(4-fluorobenzoyl)pyrrolo[1,2-c]pyrimidine-5-carboxylate (P376): yellow crystals; 0.56 g (50 %). IR (cm-1): 2949, 1697, 1618, 1597, 1505, 1476, 1411, 1330, 1270, 1229, 1197, 1151,1084. 1H NMR (300 MHz, CDCl3) δ:1.43 (t, 3H, J = 7.1 Hz, Me); 3.95, 4.01 (2s, 6H, 2MeO); 4.41 (q, 2H, J = 7.1 Hz, CH2); 6.96 (d, 1H, J = 8.4 Hz, H-5'); 7.21 (t, 2H, J = 8.5 Hz, H-3", H-5"); 7.70 (d, 1H, J = 2.1 Hz, H-2'); 7.73-7.76 (m, 3H, H-6', H-6); 7.85-7.90 (m, 2H, H-2", H-6"); 8.50 (d, 1H, J = 1.5 Hz, H-4); 10.49 (d, 1H, J = 1.5 Hz, H-1); 13C NMR (75 MHz, CDCl3) δ: 14.6 (Me); 56.1 (2MeO); 60.6 (CH2); 106.7 (C-5); 107.4 (C-4); 109.8 (C-2'); 111.3 (C-5'); 115.7 (J= 22.0 Hz, C-3", C-5"); 119.9 (C-6'): 122.0 (C-7); 129.4 (C-1'); 129.9 (C-6);131.5 (J= 8.1 Hz, C-2", C-6") 140.7 (C-1);135.3, 141.2, 149.4, 149.8, 151.1 (C-3, C-4a, C-3', C-4', C-1"); 165.1 (J = 251.9 Hz, C-4"); 163.7 (CO2Et); 183.7 (COAr). Anal. Calcd. for C25H21FN2O5(448.44): C 66.96, H 4,72, N 6.25. Found C 66.89, H 4.67, N 6.31.

Diethyl 3-(3,4-dimethoxylphenyl)-7-(3-nitrobenzoyl)pyrrolo[1,2-c]pyrimidine-5,6-dicarboxylate (P311): yellow crystals; 0.57 g (43 %). IR (cm-1) : 2991, 1731, 1689, 1617, 1531, 1504, 1435, 1401, 1384, 1348, 1331, 1256, 1222, 1200. 1H NMR (300 MHz, CDCl3) δ: 1.09, 1.38 (2t, 6H, J = 7.1 Hz, 2CH3); 3.98, 4.04 (2s, 6H, 2MeO); 3.70, 4.39 (2q, 4H, J = 7.1 Hz, 2CH2); 7.00 (d, 1H, J = 8.4 Hz, H-5'); 7.70 (t, 1H, J = 8.00 Hz, H-5"); 7.71-7.78 (m, 2H, , H-2', H-6'); 8.08-8.10, 8.45-8.47 (2m, 2H, H-4", H-6"); 8.59 (t, 1H, J = 1.1 Hz, H-2"); 8.60 (d, 1H, J = 1.5 Hz, H-4); 10.40 (d, 1H, J = 1.5 Hz, H-1); Anal. Calcd. for C28H25N3O8 (531.51): C 63.27, H 4.74, N 7.91. Found C 63.38, H 4.68, N 7.82.

Ethyl 3-(3,4-dimethoxylphenyl)-7-(2,4-dimethoxybenzoyl)pyrrolo[1,2-c]pyrimidine-5-carboxylate (P552): yellow crystals; 0.57 g (47 %). (IR (cm-1): 1692, 1619, 1599, 1476, 1329, 1266, 1200.1H NMR (300 MHz, CDCl3) δ: 1.42 (t, 3H, J = 7.1 Hz, Me); 3.84, 3.96, 4.00, 4.03 (4s, 12H, 4MeO); 4.40 (q, 2H, J = 7.1 Hz, CH2);6.57 (s, 1H, H-3");6.99 (d, 1H, J = 8.4 Hz, H-5'); 7.73 (d, 1H, J = 2.1 Hz, H-2'); 7.76-7.79 (m, 3H, H-6', H-5", H-6"); 7.53 (s, 1H, H-6); 8.46 (d, 1H, J = 1.5 Hz, H-4); 10.52 (d, 1H, J = 1.5 Hz, H-1); 13C NMR (75 MHz, CDCl3) δ: 14.5 (Me); 56.0, 56.1, 56.2, 56.4 (4MeO); 60.4 (CH2); 96.7 (C-3");106.6 (C-5); 107.4 (C-4); 109.8 (C-2'); 111.2 (C-5'); 119.9 (C-6'):122.5 (C-7); 130.2, 133.7 (C-6, C-5", C-6");140.7 (C-1);101.9, 129.4, 141.0, 149.3, 149.8, 150.9, 158.1, 158.6 (C-3, C-4a, C-1', C-3', C-4', C-1", C-2", C-4");

163.7 (CO2Et);182.5 (COAr). Anal. Calcd. for C27H26N2O7 (490.50): C 66.11, H 5.34, N 5.71. Found C 66.20, H 5.39, N 5.60.

Dimethyl 3-(3,4-dimethoxylphenyl)-7-(2,4-dimethoxybenzoyl)pyrrolo[1,2-c]pyrimidine-5,6-dicarboxylate (P585): yellow crystals; IR (cm-1) : 1701, 1610, 1504, 1475, 1329, 1267, 1199. 1H NMR (300 MHz, CDCl3) δ: 3.47, 3.81, 3.89, 3.98, 3.99, 4.04 (6s, 18H, 6MeO); 6.49 (s, 1H, H-3"); 7.01 (d, 1H, J = 8.4 Hz, H-5'); 7.73 (d, 1H, J = 2.1 Hz, H-2'); 7.76-7.79 (m, 3H, H-6', H-5", H-6"); 8.52 (d, 1H, J = 1.5 Hz, H-4); 10.49 (d, 1H, J = 1.5 Hz, H-1); 13C NMR (75 MHz, CDCl3)δ: 51.9, 52.6, 56.0 (2C) 56.1, 56.4 (6MeO); 96.0 (C-3"); 107.3 (C-4); 109.8 (C-2'); 111.1 (C-5'); 120.0 (C-6'): 122.8 (C-7); 133.2, 133.4 (C-5", C-6"); 139.8 (C-1); 101.2, 104.2, 120.6, 129.0, 140.5, 149.3, 150.3, 151.0, 158.7, 158.8 (C-3, C-4a, C-5, C-6, C-1', C-3', C-4', C-1", C-2", C-4");162.9, 164.6 (2CO2Me);182.8 (COAr). Anal. Calcd. C26H24N2O5: C 70.26, H 5.44, N 6.30. Found C 70.42, H 5.65, N 6.17.

Dimethyl 3-(3-methylphenyl)-7-(3-nitrobenzoyl)pyrrolo[1,2-c]pyrimidine-5,6-dicarboxylate (P565): yellow crystals; 0.52 g (44 %). IR (cm-1): 2955, 1747, 1709, 1620, 1600, 1530, 1496, 1447, 1424, 1387, 1339, 1248, 1209, 1119. 1H NMR (300 MHz, CDCl3) δ: 2.47 (s, 3H, Me); 3.92 (s, 6H, 2MeO); 7.31-7.33 (m, 1H, H-4'); 7.42 (t, 1H, J = 7.6 Hz, H-5'); 7.70 (t, 1H, J = 8.0 Hz, H-3");7.95-7.99 (m, 3H, H-2', H-6');8.03-8.06 (m, 1H, H-6"); 8.43-8.46 (m, 1H, H-4");8.56 (t, 1H, J = 1.8 Hz, H-2"); 8.61 (d, 1H, J = 1.5 Hz, H-4); 10.38 (d, 1H, J = 1.5 Hz, H-1).13C NMR (75 MHz, CDCl3) δ: 21.5 (Me); 52.0, 52.5 (2MeO); 105.3 (C-5); 108.6 (C-4); 123.5, 124.2 (C-4', C-4"); 126.4, 131.1, 134.2 (C-2", C-5", C-6"); 127.7, 129.0, 129.5 (C-2', C-5', C-6'); 119.1, 133.6, 136.0, 138.9, 140.2, 140.3, 151.3 (C-4a, C-6, C-7, C-1', C-1", C-3', C-3");140.1 (C-1);147.7 (C-3);162.6, 164.3 (2COO); 183.4 (COAr). Anal. Calcd. for C25H19N3O7 (473.43): C 63.42, H 4.05, N 8.87. Found C 63.35, H 4.13, N 8.76.

CHAPTER 6
SPECTRAL STUDIES OF PIROLOPIRIMIDES

6.1. SPECTRAL STUDIES OF 3-BIPHENIL PYRROLO[1,2-*c*]PYRIMIDINES

6.1.1. Absorbance study of 3-biphenylpyrrolo[1,2-c]pyrimidine derivatives

UV-VIS spectra of the compounds have been recorded in order to evaluate the excitation wavelength for the study of the pyrrolo[1,2-*c*]pyrimidine framework fluorescence. Acetonitrile:chloroform mixture (1:1) has been found the appropriate solvent. For instance Fig. 6.1A shows the obtained spectra at increasing concentrations of compound **4d** in acetonitrile:chloroform (1:1) and Fig. 6.1B shows the linear dependences on concentration of the recorded absorbances at the main maximum wavelengths λ_{max1} = 268 nm and λ_{max2} = 384 nm. The extinction coefficients (ε_1, ε_2) at the two wavelengths (λ_{max1} and λ_{max2}) have been calculated from the slopes of the linear dependences of absorbance on concentration, and they are shown in Fig. 6.1B.

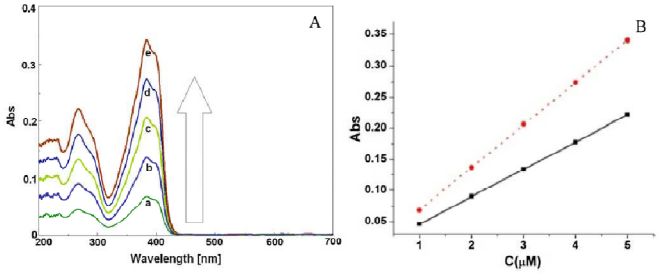

A B

Figure 6.1. A: Spectra of **4d** in acetonitrile:chloroform (1:1) at increasing concentrations (μmol/L)**:** 1 (a), 2 (b), 3 (c), 4 (d), 5 (e) **B:** Linear dependences of the absorbance on concentration for **4d** at λ_{max1}= 268 nm (solid line) and λ_{max2}= 384 nm (dotted line)

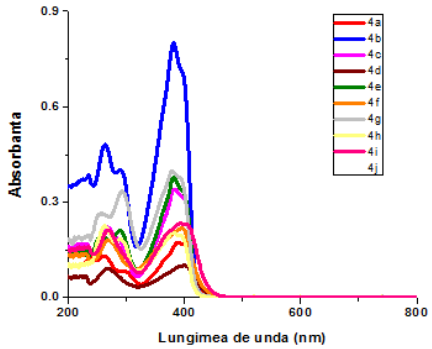

Figure 6.2. Absorption spectra for compounds **4a-j** in 5 μmol/L solutions acetonitrile:chloroform (1:1)

Figure 6.2 shows the absorption spectra for all compounds **4a-j** at the same concentration (5 μmol/L) in acetonitrile:chloroform (1:1)**.** It can be seen that absorption maxima show big differences in intensity varying between 0.1 and 0.8 for the investigated structures. All spectra have two main absorption maxima λ_{max1}, in the range 262-280 nm, and λ_{max2}, in the range 366-398 nm. The extinction coefficients (ε_1, ε_2) at the two maximum wavelengths (λ_{max1} and λ_{max2}) have been calculated for all compounds from the slopes of the linear dependences in a similar way as shown in Fig. 6.1B for **4d**. The results are summarized in Table 6.1 where are given also the equations for the linear dependences of the absorbances at λ_{max1} and λ_{max2} on concentration (**[I]**) ($A_{\lambda max1}$and $A_{\lambda max2}$ *vs* **[I]** respectively).

Table 6.1. Characteristics of the absorption spectra for compounds **4a-j** in acetonitrile:chloroform(1:1)

Compound	**λ_{max1}** (nm)	**ε** L/(mol*cm)	**Equation** $A_{\lambda max1}$ *vs* [I], *(R^2)	**λ_{max2}** (nm)	**ε** L/(mol*cm)	**Equation** $A_{\lambda max2}$ *vs* [I], *(R^2)
4a	293	49337	49337*[I] + 0.004 R^2 = 0.9994	386	105456	105456*[I] + 0.002 R^2 = 0.9999
4b	263	25640	25640*[I] + 0.001 R^2 = 0.9991	389	34200	34200*[I] + 0.001 R^2 = 0.9992
4c	262	87480	87480*[I] + 0.044 R^2 = 0.9914	381	144430	144430*[I] + 0.078 R^2 = 0.9935
4d	266	43920	43290*[I] + 0.02 R^2 = 0.9999	384	68180	68180*[I] R^2 = 0.9999
4e	270	18880	18880*[I] + 0.003 R^2 = 0.9953	399	20706	20706*[I] + 0.004 R^2 = 0.9943
4f	290	38272	38272*[I] - 0.004 R^2 = 0.9833	383	68795	68795*[I] - 0.01 R^2 = 0.979
4g	268	34200	34200*[I] + 0.013 R^2 = 0.984	398	44780	44780*[I] + 0.003 R^2 = 0.9842
4h	262	65250	65250*[I] + 0.005 R^2 = 0.998	380	77820	77820*[I] + 0.005 R^2 = 0.9979
4i	292	39784	39784*[I] - 0.003 R^2 = 0.9994	380	34836	34836*[I] + 0.003 R^2 = 0.9999
4j	260	40740	40740*[I]+0.0155 R^2 = 0.987	381	44950	44950*[I]+0.0131 R^2 = 0.9885

* correlation coefficient

Fig. 6.2 shows that the nature of substituents R connected to the pyrrolo[1,2-*c*]pyrimidine framework induces significant differences in their spectra. R nature has an important influence both on λ_{max} and ε. The replacement of fluorine atom (from compound **4c**) with a bromine atom (in compound **4d**) and chlorine atom (in compound **4a**) induces a bathochromic shift (to higher wavelengths) of λ_{max1} and λ_{max2}; this is the effect of electronegativity of the atoms. By comparing the compound **4h** with **4i** it can be concluded that the hypsochromic shift (to lower wavelengths)

for compound **4h** is caused by the disturbance of conjugation due to deviation from co-planarity of the aromatic rings imposed by steric impediments.

6.1.2. Fluorescence study of 3-biphenylpyrrolo [1,2-c] pyrimidine derivatives

The emission spectra of compounds **4a-j** were recorded in acetonitrile:chloroform (1:1) solutions. For each compound the spectra were recorded at the corresponding absorption maxima λ_{max1} and λ_{max2} (Table 6.1). The emission spectra for λ_{max1} have fluorescence intensities smaller (less than 50%) than for λ_{max2} (Fig. 6.3). The spectra obtained at the same concentration with excitation at λ_{max2} are shown in Fig. 6.4.

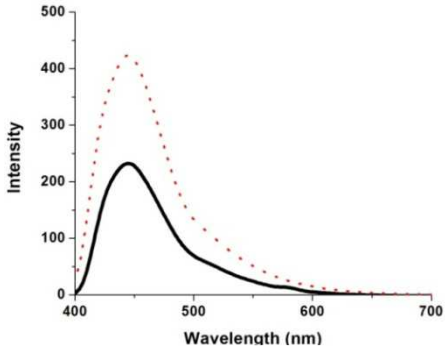

Figure 6.3. Emission spectra of compounds **4f** for excitation at λ_{max1} = 290 nm (solid line) and λ_{max2} = 380 nm (dot line) in solutions (10^{-6} mol/ L) in acetonitrile:chloroform (1:1);

All compounds present one single emission band in the blue range domain (430 – 465 nm) as seen also in Table 6.2. The spectra in Fig. 6.4 have been grouped in 3 categories (A, B, C), in agreement with the compounds structure: **4c-f** (A), **4g-i** (B), **4a-b** (C), and the values of their fluorescence intensity are given at the end of discussion. Studies regarding their fluorescence characteristics (Stokes shift, quantum yield and fluorescence quenching) have been performed.

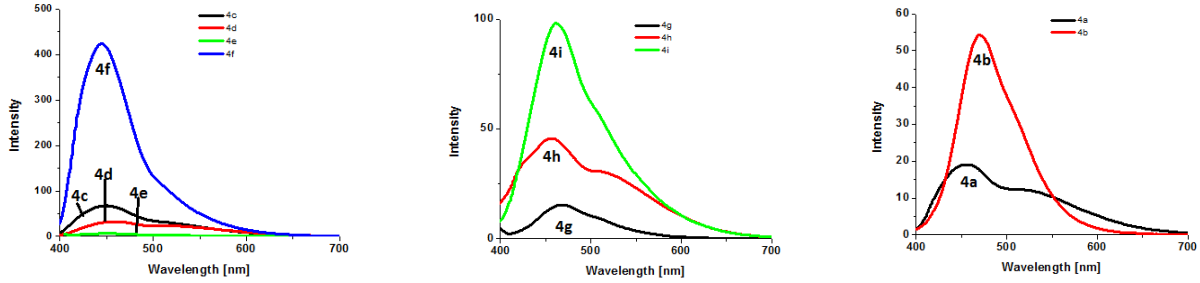

A **B** **C**

Figure 6.4. Emission spectra of compounds **4c-f** (A), **4g-i** (B), **4a-b** (C) in solutions (10^{-6}mol/ L) in acetonitrile:chloroform (1:1); each spectrum has been recorded for excitation at the specific wavelength λ_{max2} (given in Table 6.1)

The fluorescence and the related properties of the pyrrolo[1,2-*c*]pyrimidine derivatives **4a-i** certainly is influenced by the nature of the substituents and this is discussed further. When comparing the compounds **4c, 4d, 4e** and **4f** of the group A (in which R is a substituted phenyl in position 4 with F, Br, NO_2 and $(MeO)_2$, respectively), it can be noticed that their fluorescence varies in the order **4f** > **4c** > **4d** > **4e**; this order corresponds to the influence of the following substituents: MeO > F > Br > NO_2. Compound **4f** has the highest fluorescence intensity; witch can be attributed to the presence of the two repulsive methoxy groups. Compound **4c** presents a lower degree of fluorescence then **4d** due to the smaller volume of the fluorine atom (in compound **4c)** in comparison with bromine atom (in compound **4d)**. This is an example of the *heavy atom effect* (Guilbault, 1973), which suggests that the probability of intersystem crossing increases as the size of the molecule increases. The presence of bromine atom (compound **4d**), leads to a loss of excitation energy by collision between molecules due to its big volume, which is the consequence of the fluorescence intensity decrease.

In the group B, **4i**, **4h** and **4g** wich have biphenyl, 2-naphtyl and 4-nitrophenyl as substituent R and $R^1 = R^2$, compound **4g** presents the lowest fluorescence intensity. This might lead to the conclusion that the moieties presenting an extended degree of conjugation such as naphthyl and biphenyl induce a high degree of fluorescence. The difference between **4i** and **4h** could be explained by the free rotation of the two phenyl rings in **4h**, which can place the two phenyls out of the plane, thus decreasing the degree of conjugation and leading to a decrease in fluorescence. The lower fluorescence of **4g** compared to that of the other two structurally analogous compounds **4i** and **4h** can be attributed to an increased tendency to aggregate in solution, due to the presence of nitro group (the polarized structure of the nitro group favors the appearance of compact supramolecular structures).

The compounds **4a** and **4b** of the group C, present low fluorescence intensities due to the presence of electron withdrawing substituents such as NO_2 and Cl. The low fluorescence intensities seen in the experimental fluorescence spectra (Figure 3) are expressed also by the calculated values of fluorescence quantum yield and K_{SV} (Table 6.3).

Stokes shifts

Stokes shifts were calculated (Table 6.2) using the equation (6.1) for all compounds **4a-i** on the basis of absorption-emission properties. The equation (1) gives errors of 5-20%. The Stokes shifts were calculated at each maximum wavelength ($\Delta\tilde{\nu}_1$ and $\Delta\tilde{\nu}_2$) at the same concentration (10^{-6} mol/L). All these compounds have fluorescence in the range of 430-470 nm. The data from Table 6.2 show higher Stokes shifts for excitation at $\lambda_{max,exc1}$ in comparison to $\lambda_{max,exc2}$ for all the investigated compounds.

$$\Delta\tilde{\nu} = \frac{1}{\lambda_{max,exc}} - \frac{1}{\lambda_{max,em}} \qquad (6.1)$$

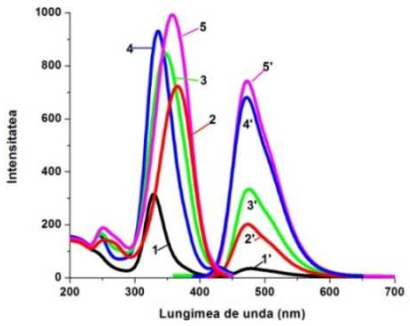

Figure 6.5. Excitation spectra (1-5) and emission spectra (1'-5 ') for compound **4j** in acetonitrile: chloroform (1: 1) at various concentrations (mol / L): 10^{-6} (1-1 '), $8x10^{-7}$ (2-2 '), $6x10^{-7}$ (3-3'), $2x10^{-7}$ (4-4 '), 10^{-7} (5-5').

Table 6.2. Maximum wavelengths of absorption ($\lambda_{max,exc}$) and emission ($\lambda_{max,em}$) and the corresponding Stokes shifts ($\Delta\tilde{\nu}_1$, $\Delta\tilde{\nu}_2$) for the compounds **4a-j** (10^{-6} mol/ L) in acetonitrile:chloroform(1:1)

Grupa	Compus	$\lambda_{max,exc1}$ (nm)	$\lambda_{max,em1}$ (nm)	$\lambda_{max,exc2}$ (nm)	$\lambda_{max,em2}$ (nm)	$\Delta\bar{\upsilon}_1$ (cm^{-1})	$\Delta\bar{\upsilon}_2$ (cm^{-1})
A	**4a**	268	453	383	454	15.238	4083
	4b	262	459	354	466	16.381	6789
	4j	262	458	329	478	16.338	9860
B	**4c**	262	462	381	463	16.552	4648
	4d	268	462	389	466	15.668	4536
	4e	270	457	400	462	15.155	3354
	4f	290	435	380	446	11.494	3894
C	**4g**	262	451	360	463	15.994	6179
	4h	263	430	380	460	14.767	4576
	4i	264	455	380	464	15.900	4764

Quantum yield

The fluorescence quantum yield (QY) is among the most important characteristics of fluorescence being defined as the efficiency of a fluorophore to convert the absorbed light into fluorescence. QY has been calculated (Table 6.3) for all compounds **4a-j** using the equation (6.2) order to evaluate their fluorescence intensity. QY was measured for diluted acetonitrile:chloroform (1:1) solutions ($3.5 * 10^{-6}$ mol/ L) using quinine sulphate as standard (Tatu et al., 2015). In (6.2): QY, A, I, n are quantum yield, maximum value of the absorbance at the emission wavelength $\lambda_{max,em2}$, area of the emission peak and refractive index for the solution of investigated compound, and QY_{ref}, A_{ref}, I_{ref}, n_{ref} are the corresponding values for the standard solution respectively. The following values are constant: n =1.3942, and I_{ref} = 16463; n_{ref} = 1.339; QY_{ref} = 0.6 (for the quinine sulphate standard solution) in the case of diluted solutions of all compounds **4a-i** in acetonitrile:chloroform (1:1).

$$QY = QY_{ref} \times \frac{I}{A} \times \frac{A_{ref}}{I_{ref}} \times \frac{n}{n_{ref}} \qquad (6.2)$$

Fluorescence quenching

The fluorescence quenching of the new synthesized pyrrolo[1,2-*c*]pyrimidines in presence of the quencher 1,4-benzoquinone (BQ) has been examined. This is a very important property of a specific chromophore which may lead to interesting applications in the investigation supramolecular assemblies for example. The fluorescence quenching curves for compounds **4a-j** in presence of BQ have been recorded. For instance Fig.6.6 presents the fluorescence decrease in intensity (quenching) for the compound **4f** in presence of increasing concentrations of BQ.

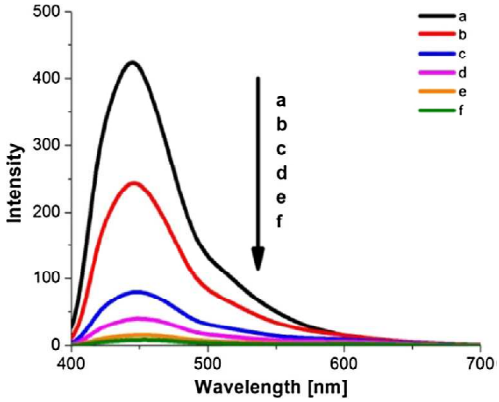

Figura 6.6. Fluorescence quenching curves of **4f** (10^{-5}mol/L) in acetonitrile:chloroform (1:1) upon addition of increasing concentrations mol/L of BQ: 0 (a), 0.006 (b), 0.012 (c), 0.018 (d), 0.024 (e), and 0.030 (f).

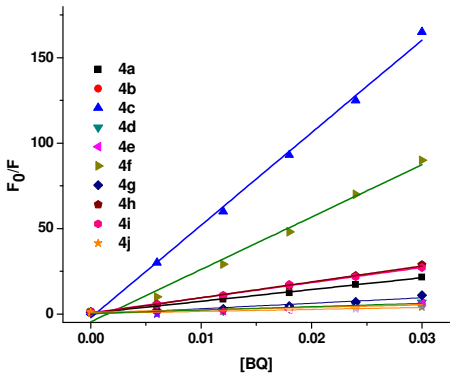

Figura 6.7. Stern-Volmer plots for benzoquinone (BQ) quenching of the studied compounds in solutions (10^{-5}mol/L) in acetonitrile:chloroform (1:1); the quenching curves have been recorded at $\lambda_{max,em2}$

The changes in the fluorescence intensity related to BQ concentration are expressed by Stern-Volmer (S-V) equation (6.3) were: F_0 = fluorescence intensity in the absence of quencher; F = fluorescence intensity in the presence of quencher; K_{SV} = Stern-Volmer constant; [BQ] = concentration of the quencher (1,4-benzoquinone).

$$\frac{F_0}{F} = 1 + K_{SV} \cdot [BQ] \qquad (6.3)$$

The ratios of F_0/F were calculated and plotted (Fig. 6.7) against [BQ], and K_{SV} were determined according to (6.3) from their slopes (Table 6.3).

Looking at the values from Table 6.3, it can be seen that two of the compounds (**4c** and **4f**) have higher values of QY and K_{SV} (their values are highlighted with bold figures in Table 6.3). These higher values of QY and K_{SV} could be the result of a π electron conjugated system expansion for this compound. This assumption is confirmed by the high values of the fluorescence quantum yield for the two compounds.

Table 6.3. Absorption and fluorescent parameters for the compounds 4a-i in acetonitrile:chloroform (1:1) solutions (3.5 * 10-7mol/ L) using quinine sulphate as standard.

Group	Compound	R	R^1	R^2	A	I	A_{ref}	QY (%)	K_{SV} (M^{-1})
C	**4a**	4-Cl	H	Me	0.05263	2146	0.03	4.64	637
	4b	3-NO_2	H	Me	0.059	4025	0.0248	6.42	223
A	**4c**	4-F	H	OEt	0.04859	6479	0.0376	**19.02**	**5748**
	4d	4-Br	H	OEt	0.0867	3750	0.0387	6.35	206
	4e	4-NO_2	H	OEt	0.06875	166	0.02	0.18	202
	4f	3,4-diMeO	H	OEt	0.079	29733	0.0387	**55.27**	**2942**
B	**4g**	4-NO_2	CO_2Me	OMe	0.03223	989	0.0298	3.47	249
	4h	4-C_6H_5	CO_2Et	OEt	0.06017	3380	0.0418	8.91	749
	4i	3,4-benzo	CO_2Et	OEt	0.08411	8152	0.0418	15.37	987

6.2. SPECTRAL STUDIES FOR 3-PHENYLPYRROL [1,2-c] PIRIMIDINES

6.2.1. Absorbance study of 3-phenylpyrrolo [1,2-c] pyrimidine derivatives

The optical properties of compounds **3-12** (Table 6.4) have been investigated by absorbance and fluorescence spectroscopy in their solution. The compounds have been grouped in 2 categories (A, B), in agreement with their structure: R_4 is an ester group (COOMe or COOEt) for compounds of the type A, and R_4 = H for compounds of the type B. All their spectra display two main absorption maxima, λ_{abs1} (in the range 241 - 275 nm), and λ_{abs2} (in the range 390 - 405 nm), corresponding to the n→π* and π→π* transitions, respectively, as shown in Figure 6.8 for the spectra recorded in chloroform solutions. The significant differences in the absorption spectra are induced by the nature of the substituents R_1, connected to the benzene ring from the position 3 of the pyrrolo[1,2-*c*]pyrimidine core or the substituent R_2, connected to the benzoyl moiety attached at C-7.

Table 6.4. The investigated pyrolo[1,2-*c*]pyrimidine derivatives

Cod	Compound	R_1	R_2	R_3	R_4	m.p. (^oC)
		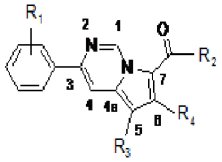				
3	P319	2-MeO	fenil	CO_2Me	CO_2Me	180-182
4	P335	3-MeO	3-NO_2-fenil	CO_2Et	CO_2Et	209-211
5	P338	2,4-diMeO	4-Br-fenil	CO_2Me	CO_2Me	197-199
6	P563	2,4-diMeO	4-Me-fenil	CO_2Et	H	106-108
7	P376	3,4-diMeO	4-F	CO_2Et	H	223-225
8	P543	3,4-diMeO	4-Me-fenil	CO_2Et	H	221-223
9	P311	3,4-diMeO	3-NO_2-fenil	CO_2Et	CO_2Et	166-168
10	P552	3,4-diMeO	2,4-diMeO-fenil	CO_2Et	H	237-239
11	P585	3,4-diMeO	2,4-diMeO-fenil	CO_2Me	CO_2Me	163-164 [60]
12	P565	3-Me	3-NO_2-fenil	CO_2Me	CO_2Me	195-199 [60]

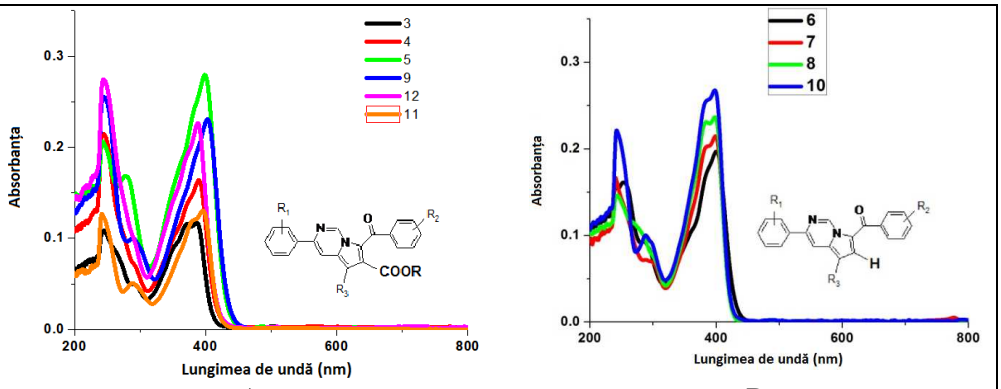

A B

Figure 6.8. Absorbtion Spectra of de pyrrolo[1,2-*c*]pyrimidine derivatives in chloroform (5 μM).

6.2.2. Fluorescence study of 3-phenylpyrrolo [1,2-c] pyrimidine derivatives

The main absorption and fluorescence characteristics: the wavelength for the maximum absorption band (λ_{abs}), extinction coefficient (ε), wavelength for the maximum emission (λ_{em}), Stokes shift ($\Delta\tilde{\nu}$), quantum yield (QY) and Stern-Volmer constant (K_{SV}) have been calculated for compounds **3-12** in chloroform as shown in the previous papers. They are summarized in Table 6.5. Absorption and fluorescence parameters in other solvents (CH_2Cl_2, CH_3CN, DMSO) for compounds **3-12** are given in Table 6.6. It can be seen that the absorption maxima are different in the investigated solvents.

The emission spectra of pyrrolo[1,2-c]pyrimidine derivatives were recorded in all solvents with excitation light at the corresponding absorption maxima λ_{abs1} and λ_{abs2} given in Tables 6.5 and 6.6. The emissions corresponding to λ_{abs1} have smaller intensities, less than 50% (inset Figure 6.9B) than those corresponding to λ_{abs2}. The emission spectra of the compounds **3-12** measured for λ_{abs2} at the same concentration are shown in Figures 6.9A and 6.9B for chloroform solutions (Figure 6.9) and they have been considered for the calculation of fluorescence parameters. The studied compounds show a single emission band in the blue region (436–463 nm) of the visible spectrum (Figure 6.9).

The emission wavelengths and intensities are influenced by the nature of the substituents linked to the pyrrolo[1,2-c]pyrimidine moiety, which is the fluorophore.

When comparing the results summarized for the compounds from the group A (R4=CO_2Me, CO_2Et) with the compounds from the group B (R4= H), it can be concluded that the presence of an ester attached to C-6 of the pyrrole moiety (in case of B) induces a steep decrease in the fluorescence intensity (Figure 6.9). This lead to lower quantum yields for compounds of the type A in respect to the compounds of type B (in Table 6.5 the compounds of the type A are in pink color, where those of type B in blue). The same behavior has been noticed in all solvents (Table 6.6) where QY values are higher for B compounds than for A. This is explained by the steric hindrance given by the ester group, which influences the conjugation between the pyrrolopyrimidine core and the benzoyl moiety at C-3 through the carbonyl bond leading to a decrease of electron delocalization reducing the influence of the substituents on the benzoyl moiety)

The data from Table 6.5 show that change of R_1, R_2 and R_3 substituents, induces significant differences in the values of luminescence characteristics like λ_{abs}, λ_{em}, ε, QY (Figure 6.10) and K_{SV}. They will be discussed further.

In order to assess the influence of substituent on the R_2, QY values were compared for compounds **7** and **8**, which have the same substituents R_1, R_3, R_4, but different R_2. From the comparison of the results obtained for these compounds the effect of the substituent R_2 on QY can be appreciated. Note that by replacing the fluorine atom (4-F in **7**) with a methyl group (4-Me in **8**) the fluorescence quantum yield QY increased twofold.

If R_2 is 4-Me (with an inductive electron donating effect $+I_s$) an increase in conjugation is produced due to the fluorophore F2, that leads to a higher value of QY for **8** (61.35) relative to **7** (38.26), where R_2 is 4-F, with a strong electron withdrawing inductive effect $-I_s$, and also an electromeric effect, $+E_s$. The explanation is also confirmed by the comparison of compounds 10 and **8**, because in compound **10** the two OMe groups have a donor effect more pronounced than that of Me group.

From the comparison of compounds **11** and **12** (with the same R_3 = COOMe), but with different R_1 and R_2, there is a large difference between the values for QY: 29.46% for **11** and 3.24% for **12**.

By introducing a second OMe group at the 4-position of the phenyl ring (attached to the heterocyclic ring) in compound **9** compared to compound **4** with a 3-MeO the conjugation on the F1 fluorophore is more favored, being expected an increase in fluorescence, as the length of the conjugated system increases: 2.64% (for **4**) and 2.99% (for **9**).

The change of R_1 substituent position on the phenyl ring (attached to the heterocyclic ring at position 3) yields important fluorescence variations. The decrease of the QY value for **6** (51.77%) relative to **8** (61.35%) can be explained by the steric constraint that diminishes the F1 fluorophore conjugation due to the OMe group at position 2.

Considering that the influence of the R_3 substituent (COOMe and COOEt) is small, as shown above, the comparison of compounds **9** and **11** which have the same R_1, but different R_2, show that the effect of the substituent R_2 is very important. Thus, for compound **11** in which R_2 has an electron-donor effect (R_2 = 2,4-diMeO), QY is 27.46%, and for **9** (R_2 = 3-NO2) QY is 2.99%. This confirms that an electron-attractive substituent leads to a decrease in fluorescence, while an electron donor substituent leads to an increase of fluorescence.

Table 6.5. Spectral characteristics of compounds 3-12 in chloroform (5 μm)

Group	**Compus**	**λ_{abs1} (nm)**	**ε_1 * L/(mol*cm)**	**λ_{abs2} (nm)**	**ε_2 * L/(mol*cm)**	**λ_{em} (nm)**	**$\Delta\tilde{\nu}_1$ (cm^{-1})**	**$\Delta\tilde{\nu}_2$ (cm^{-1})**	**QY (%)**	**K_{SV}**
A	**3**	261	44620	386	46960	463	19193	6786	11.04	307
	4	252	39520	390	50630	539	22263	6945	2.64	160
	5	242	42770	392	57930	440	22769	6510	6.63	287
	9	250	61060	395	65910	456	18070	2946	2.93	79
	11	242	25600	396	27850	450	19100	3030	27.46	644
	12	268	56200	388	47200	436	18656	7116	3.24	242
B	**6**	268	23300	396	39100	462	14326	3608	51.77	928
	7	265	25200	400	36800	462	16090	3418	38.26	367
	8	275	29090	397	47900	458	14529	3355	61.35	638
	10	258	42300	405	53800	437	15876	2306	11.70	232

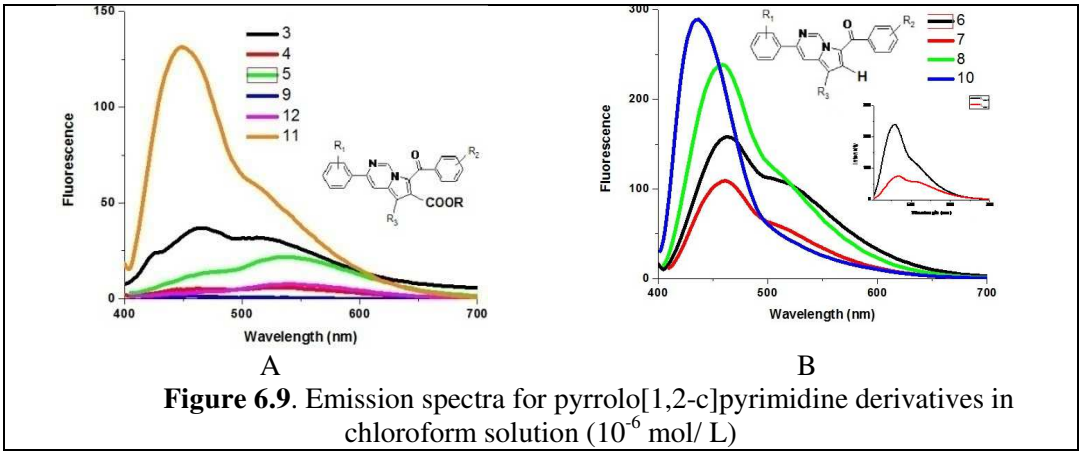

Figure 6.9. Emission spectra for pyrrolo[1,2-c]pyrimidine derivatives in chloroform solution (10^{-6} mol/ L)

When comparing the results summarized for the compounds from the group A (R_4=CO_2Me, CO_2Et) with the compounds from the group B (R_4= H), it can be concluded that the presence of an ester attached to C-6 of the pyrrole moiety (in case of B) induces a steep decrease in the fluorescence intensity (Figure 6.10). This lead to lower quantum yields for compounds of the type A in respect to the compounds of type B (in Table 6.4 the compounds of the type A are in pink color, where those of type B in blue). The same behavior has been noticed in all solvents (Table 6.5) where QY values are higher for B compounds than for A. : This is explained by the steric hindrance given by the ester group, which influences the conjugation between the pyrrolopyrimidine core and the benzoyl moiety at C-3 through the carbonyl bond leading to a decrease of electron delocalization reducing the influence of the substituents on the benzoyl moiety)

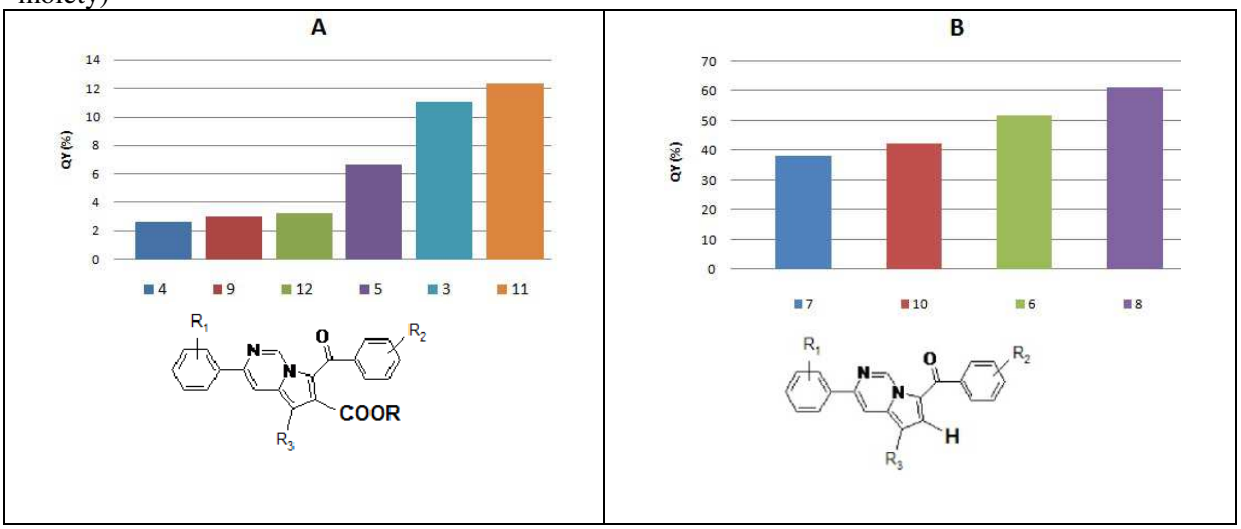

Figure 6.10. Compared quantum yields for the compounds **3**-**12** of the type A and B.

The data from Table 6.4 show that change of R_1, R_2 and R_3 substituents, induces significant differences in the values of luminescence characteristics like λ_{abs}, λ_{em}, ε, QY (Figure 6.9) and K_{SV}. They will be discussed further.

In order to assess the influence of substituent on the R_2, QY values were compared for compounds **7** and **8**, which have the same substituents R_1, R_3, R_4, but different R_2. From the comparison of the results obtained for these compounds the effect of the substituent R_2 on QY can be appreciated. Note that by replacing the fluorine atom (4-F in **7**) with a methyl group (4-Me in **8**) the fluorescence quantum yield QY increased twofold.

If R_2 is 4-Me (with an inductive electron donating effect $+I_s$) an increase in conjugation is produced due to the fluorophore F2, that leads to a higher value of QY for **8** (61.35) relative to **7** (38.26), where R_2 is 4-F, with a strong electron withdrawing inductive effect $-I_s$, and also an

electromeric effect, $+E_s$. The explanation is also confirmed by the comparison of compounds **10** and **8**, because in compound **10** the two OMe groups have a donor effect more pronounced than that of Me group.

From the comparison of compounds **11** and **12** (with the same R_3 = COOMe), but with different R_1 and R_2, there is a large difference between the values for QY: 29.46% for **11** and 3.24% for **12**.

By introducing a second OMe group at the 4-position of the phenyl ring (attached to the heterocyclic ring) in compound **9** compared to compound **4** with a 3-MeO the conjugation on the F1 fluorophore is more favored, being expected an increase in fluorescence, as the length of the conjugated system increases: 2.64% (for **4**) and 2.99% (for **9**).

The change of R_1 substituent position on the phenyl ring (attached to the heterocyclic ring at position 3) yields important fluorescence variations. The decrease of the QY value for **6** (51.77%) relative to **8** (61.35%) can be explained by the steric constraint that diminishes the F1 fluorophore conjugation due to the OMe group at position 2.

Considering that the influence of the R_3 substituent (COOMe and COOEt) is small, as shown above, the comparison of compounds **9** and **11** which have the same R_1, but different R_2, show that the effect of the substituent R_2 is very important. Thus, for compound **11** in which R_2 has an electron-donor effect (R_2 = 2,4-diMeO), QY is 27.46%, and for **9** (R_2 = 3-NO_2) QY is 2.99%. This confirms that an electron-attractive substituent leads to a decrease in fluorescence, while an electron donor substituent leads to an increase of fluorescence.

The fluorescence quenching of the new synthesized pyrrolo[1,2-*c*]pyrimidines in presence of 1,4-benzoquinone (BQ), as fluorescence quencher, has been examined. This is a very important property of a specific chromophore which is connected to interesting applications in the investigation of supramolecular assemblies. The fluorescence quenching curves for compounds **3-12** in the presence of BQ have been recorded. The fluorescence decreases in intensity (quenching) in presence of increasing concentrations of benzoquinone [BQ], as it has been shown for instance for the compound **10** (Figure 6.11B inset). A linear Stern-Volmer plot has been obtained for **10** and all the other investigated compounds (Figure 6.11A and 6.11B, for compounds of type A and B, respectively). However, the observation of a linear Stern-Volmer plot proves that collisional quenching of fluorescence has occurred. The quenching has been calculated as the ratio F_0/F between fluorescence intensity in the absence of quencher (F_0) and fluorescence intensity in the presence of quencher (F). K_{SV} values (Tables 6.2 and 6.6) were determined from the slopes of their linear dependences.

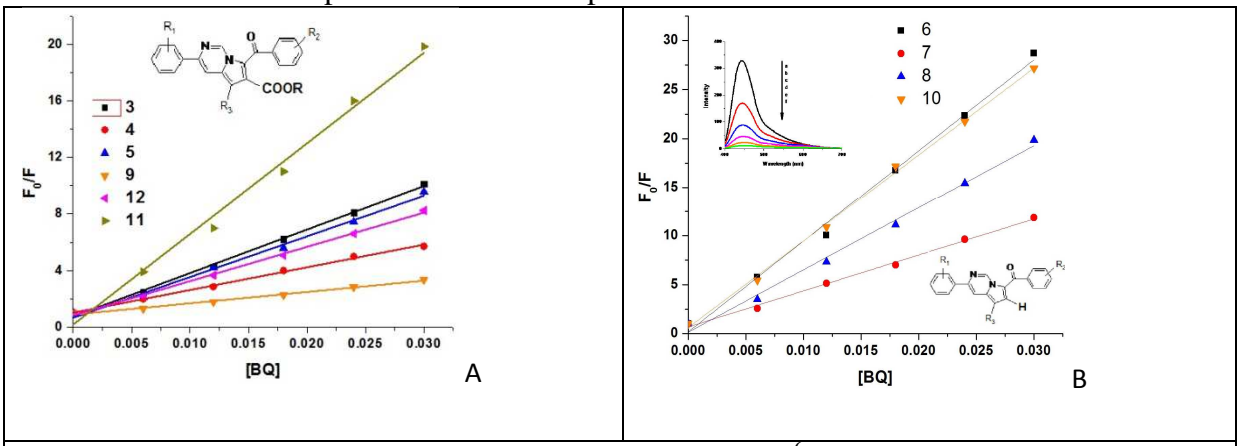

Figure 6.11. Stern-Volmer plots (F_0/F) for BQ quenching in 10^{-6} mol/L chloroform solutions of the studied compounds of type A (**3, 4, 5, 9, 11, 12**) and B (**6, 7, 8, 10**); inset Figure 4B: fluorescence decrease in intensity (quenching) in presence of increasing concentrations of benzoquinone [BQ] for compound **10**

6.2.3. Solvatocromy studies

Solvent properties, such as polarity, are known to influence the photoluminescence of organic fluorophores in solutions. Thus, the absorption and emission spectra of pyrrolo[1,2-*c*]pyrimidine derivatives were recorded in solvents with different polarity (having different dielectric constant ε) and refractive index (n): chloroform, dichloromethane, acetonitrile and DMSO. In figure 6.12 is depicted the influence of solvent polarity on the position, intensity and shape of the absorption and fluorescence bands of a representative compound **5**, this compound present the biggest red shift when the polarity of the solvent is increasing (from 440 nm in chloroform for **5** to 557 nm in DMSO for **5**). The spectral parameters of the studied compounds in different solvents are presented in Table 6.6.

Pyrrolo[1,2-*c*]pyrimidine compounds showed fluorescence quantum yields varying from 0.14 % to 87.26 % and non-monotonous dependence on solvent polarity.

The common tendency for the studied pyrrolo[1,2-*c*]pyrimidine derivatives is the bathochromic shift of the emission peaks from 4 nm (for compound 6 as seen in Table 6.5 and 6.6 line 6) to 117 nm (for compound 5 as seen in Table 6.5 and 6.6 line 3) when increasing the solvent polarity. This is a typical solvatochromic behavior for compounds that undergo an intramolecular charge transfer (ICT) upon excitation, leading to a highly polar, charge-separated emitting state, stabilized by polar solvents. The bathochromic shift of the emission maxima, seen when the solvent polarity increases, suggests that ICT for the excited state is polar, with a large dipole moment, due to a substantial charge redistribution. Hence, it is more stabilized in more polar solvents. From figure 6.12 it can be seen that, as the solvent polarity increases, the absorption spectra exhibited minor changes in shape, intensity and peak wavelengths, due to insignificant intramolecular interactions between donor and acceptor in the ground state, while the fluorescence spectra exhibit major changes.

The fluorescence changes in shape, intensity and the Stokes shifts were examined. The polarity increase leads to a red shift of the emission peaks (Tables 6.5 and 6.6), suggesting the involvement of photo induced ICT in the singlet excited state with larger dipole moment in the excited state, as expected.

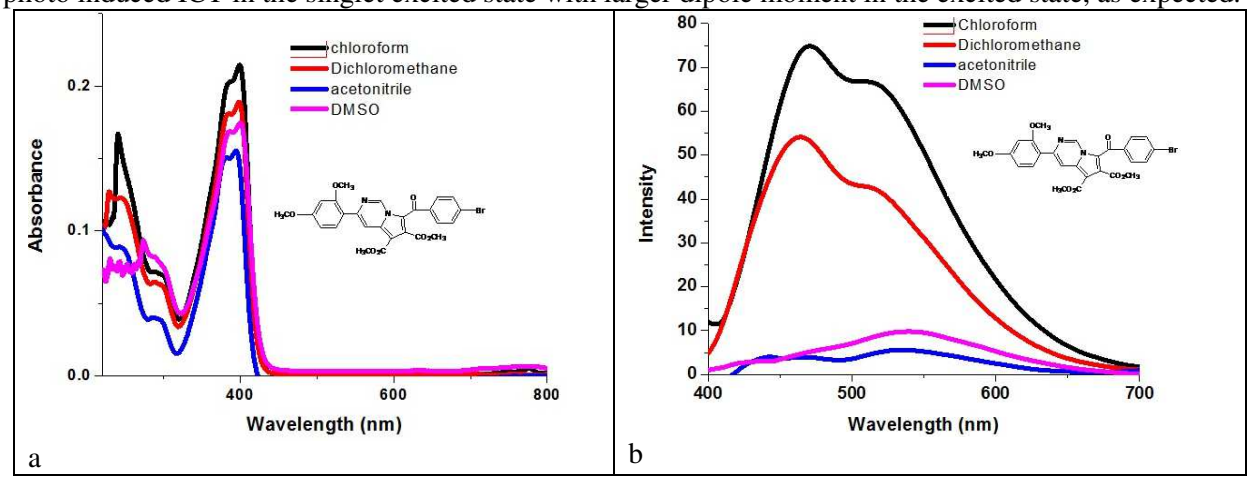

Figure 6.12. Absorption (a) and emission (b) spectra of **5** in different solvents: chloroform (black) dichloromethane (red), acetonitrile (blue), DMSO (magenta)

The Stokes shift variations are linearly correlated with the changes in the dipole moment of the molecules between the ground state and excited state; their relationship is expressed by solvent polarity functions, such as Lippert-Mataga.

Tabel 6.6. Caracteristicile spectrale ale compușilor studiați în diferiți solvenți

Groupa		CH_2Cl_2					CH_3CN					DMSO				
	Compus	λ_{abs} nm	ε L/(mol*cm)	λ_{em} nm	$\Delta\tilde{\nu}$ (cm^{-1})	QY %	λ_{abs} nm	ε L/(mol*cm)	λ_{em} nm	$\Delta\tilde{\nu}$ (cm^{-1})	QY %	λ_{abs} nm	ε L/(mol*cm)	λ_{em} nm	$\Delta\tilde{\nu}$ (cm^{-1})	QY %
A	**3**	242 394	36900 39200	470	19392 3007	0.8	248 375	21500 24800	525	21347 7691	2.88	291 378	15600 25000	457	12482 4573	4.66
	4	246 386	22900 17700	437	17767 3023	0.84	246 380	81600 59500	428	17285 2951	1.74	290 390	19600 25500	435	11494 2652	0.8
	5	245 388	21000 29800	459	19029 3986	10.07	277 391	64100 85600	555	18083 7557	0.5	290 395	18400 22400	557	16529 7363	5.64
	9	245 394	40100 37400	460	18886 3007	0.14	244 390	47300 38600	465	20019 4352	2.29	290 388	26400 44900	455	19688 34672	0.6
	12	245 387	50300 42100	457	18934 3957	1.29	245 382	43200 33600	520	21585 6947	1.64	290 385	23400 27600	536	15826 7317	2.03
	11	245 394	27800 32500	460	19927 3836	12.33	240 391	44000 38700	468	20299 4207	8.84	270 396	46300 49700	470	15760 3513	6.8
B	**6**	246 397	24300 43000	466	19191 3729	25.98	270 390	43400 29700	468	15669 4273	29.8	289 395	15500 31800	468	13234 3948	51.51
	7	244 398	122800 197100	466	19524 3666	5.67	244 395	17600 27600	469	19661 3994	10.7	290 390	14000 31600	470	20390 4364	21.74
	8	266 397	89000 148600	468	16226 3821	20.99	266 393	20900 39600	481	16226 4077	52.6	292 390	25000 49300	492	12833 4227	87.26
	10	240 402	34100 44100	438	18835 2284	17.9	252 400	44300 83100	439	16903 2666	3.89	295 395	13200 40300	467	11476 3219	40.16

The changes in the dipole moment have been calculated by applying Lippert-Mataga method. The difference in dipole moments ($\Delta\mu$) upon excitation has been calculated from the slope of the linear dependences between Stokes shifts and the solvent polarity function (Δf). In Figure 6.13 the values for compound **8** are presented, as representative compound. It has been selected as representative due to its smaller value of the difference in dipole moments as seen in Table 6.7), where are given the dipole moment of the ground state (μ_g) and in the excited state (μ_e). The value of the R^2 factor (0.973) for the linear dependence in Figure 6.13 indicates a good correlation.

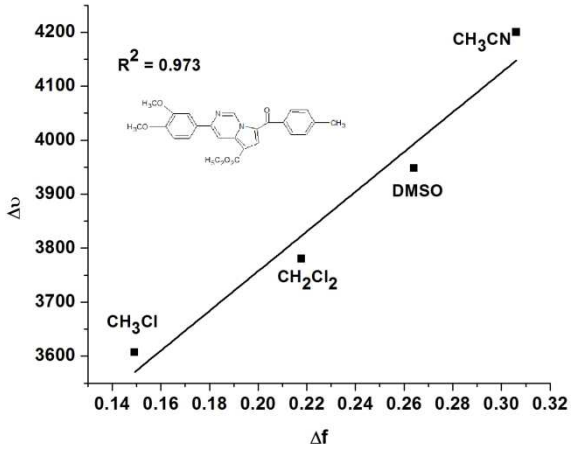

Figure 6.13. Lippert-Mataga plot ($\Delta\upsilon$ *vs* Δf) for compound **8**

Bakhshiev's and Kawski-Chamma-Viallet equations have been applied to determine the dipole moments for the ground and excited states, by plotting the solvent polarity function F_1 *vs* Stokes shift and the average sum of the absorption-emission maxima *vs* F_2 (Figures 6.14 and 6.15).

Table 6.7. Calculated dipole moments for compounds **3**-**12** using Lippert-Mataga method and Bakhshiev's and Kawski-Chamma-Viallet equations

Group	Compound	$\Delta\mu$ (D)	μ_g (D)	μ_e (D)
A	**3**	10.24	3	13.24
	4	0.82	4.06	4.89
	5	11.84	4.35	16.17
	9	5.32	4.15	9.48
	11	4.88	2.63	7.52
	12	9.27	0.2	9.68
B	**6**	3.64	2.83	6.47
	7	5.21	2.42	7.64
	8	0.38	4.32	4.7
	10	2.08	3.11	5.16

Figure 6.15 presents the linear dependence of $\tilde{\nu}_{abs} + \tilde{\nu}_{em}$ versus the solvent polarity (F_2) for the compound **8,** using the Kawski–Chamma–Viallet equation. The correlation coefficients (R^2 = 0.614) obtained is small. One reason for this value can be attributed to the specific solute/solvent interaction . When the dipole moment of the solute in the excited state is larger than in the ground state, which means the excited state is better stabilized relatively to the ground state in a more polar solvent.

Overall solvent effects on absorption and emission spectra of the pyrrolo[1,2-*c*]pirimidine derivatives were analyzed by Kamlet-Taft solvatochromic equation:

The solvents parameters: polarity/polarizability (π*), acidity (α), and basicity (β), which contribute to the overall solvent polarity, are presented in Table 6.8. The results obtained from multiple linear regression analysis are presented in Tables 6.9 and 6.10.

Table 6.9. Multilinear regression of solvatochromic parameters for compounds **3**-**12** using Stokes shifts as relevant property

Type	Compound	$10^{-3} \cdot \upsilon_0$ (cm^{-1})	$10^{-3} \cdot s$ (cm^{-1})	$10^{-3} \cdot b$ (cm^{-1})	$10^{-3} \cdot a$ (cm^{-1})
A	**3**	11.18	10.72	-3.66	4.55
	4	14.95	5.38	-2.05	1.56
	5	1.65	29.07	-12.37	6.93
	9	19.66	3.12	-2.39	1.78
	11	19.01	-0.50	0.47	-0.29
	12	47.41	-34.48	11.58	-12.80
B	**6**	32.41	-14.63	4.72	-5.71
	7	31.64	-13.62	4.29	-5.13
	8	44.87	-34.41	10.66	-13.28
	10	11.18	10.72	-3.66	4.55

The results obtained using Kamlet-Taft model indicate that the solvent effects on pyrrolo[1,2-*c*]pyrimidine derivatives fluorescence spectra are very complex. The data obtained from de multiple linear regresion are in good acordance with the experimental data. The derivatives with positive coefficients *s* and *a* present positive solvatochromism, bathocromic shift when the polarity of the solvent increases. This means that a stabilization of the electronic excited state relatively to the ground state accurs. The negative sign of the coefficient *b* indicates a hypsochromic shift, which suggests stabilization of the ground state relatively to the electronic excited state. The percentege of solvatochromic parameters are presented in Table 6.10. The obtained values indicate that the solvatochromism is more influenced by the solvent polarizability (P_{π^*}). The hydrogen-bond acidity or basicity of the solvents display small influences on the solvatochromic properties of compounds **3**-**12**. The degree of correlation between Eq. 9 and experimental data is shown in Figure 6.16 for all the investigated compounds. A good correlation (R^2= 0.9963) between the calculated and experimental υ values has been observed for all compounds.

Table 6.10. Percentage contribution of solvatochromic parameters from Eq. (9)

Type	Compound	R_1	R_2	R_3	$P_{□□}$ (%)	$P_{□}$ (%)	$P_{□}$(%)
A	**3**	2-MeO	H	CO_2Me	56.64	19.31	24.04
	4	3-MeO	3-NO_2	CO_2Et	59.83	22.85	17.30
	5	2,4-diMeO	4-Br	CO_2Me	60.10	25.56	14.32
	9	3,4-diMeO	3-NO_2	CO_2Et	42.80	32.74	24.45
	11	3,4-diMeO	2,4-diMeO	CO_2Me	39.87	37.34	22.78
	12	3-Me	3-NO_2	CO_2Me	58.57	19.67	21.74
B	**6**	2,4-diMeO	4-Me	CO_2Et	58.38	18.84	22.77
	7	3,4-diMeO	4-F	CO_2Et	59.12	18.60	22.26
	8	3,4-diMeO	4-Me	CO_2Et	58.98	18.26	22.75
	10	3,4-diMeO	2,4-diMeO	CO_2Et	60.80	21.14	18.04

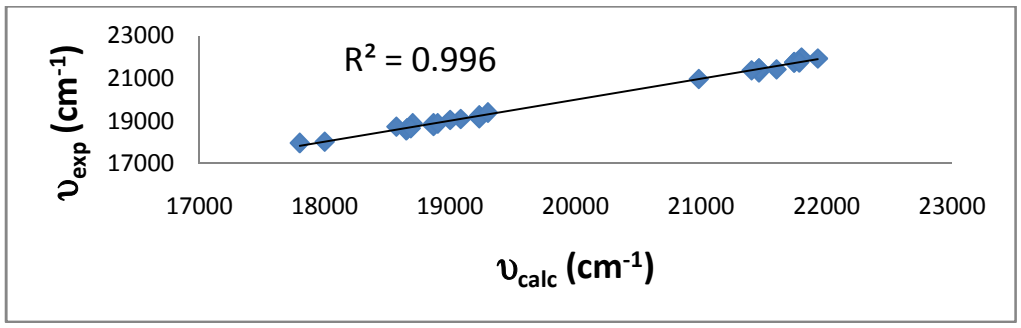

Figure 6.16. Experimental *vs*. calculated values of υ

CHAPTER 7
ELECTROCHEMICAL STUDIES OF SEVERAL PIROLOPIRIMIDINES

7.1. ELECTROCHEMICAL CHARACTERIZATION OF SEVERAL PIROLOPIRIMIDINE

Electrochemical methods used in electrochemical characterization are: cyclic voltammetry (CV), differential pulse voltammetry (DPV), voltammetry on rotating disc electrode (RDE). The anode and cathode curves were recorded at different concentrations for each compound. Both anodic and cathodic fields were obtained which were read and subsequently identified and assigned to specific electrochemical processes in the structures of the pyrrolopyrimidine compounds.

7.1.8. Electrochemical characterization for ethyl 3- (3,4-dimethoxyphenyl) -7- (2-naphthoyl) -pyrrolo [1,2-c] pyrimidine 5-carboxylate (P545)

Figure 7.50 shows the structure of pyrrolopyrimidine (**P545**)

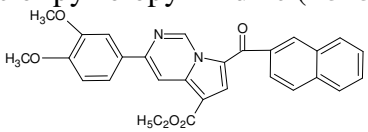

Figure 7.50 Structure of pyrrolopyrimidine **P545**

Figure 7.51 shows CV and DPV curves at different concentrations in 0.1 M TBAP, CH_3CN. Concentrations were obtained by dilution from the initial solution of 0.75 mM, which is the highest concentration of **P545** in this characterization. The anode and cathode curves were recorded starting from the stationary potential.

The DPV curves obtained at different concentrations have five oxidation peaks (numbered a1 - a5 in Figure 7.51) and four reduction peaks (numbered c1 - c4), in order of their occurrence in anodic and cathodic packs. On CV curves, just a little anodic (a1) is obvious, the other peaks appear as shoulders. The three cathode peaks c1-c3 in DPV are seen as shoulders in CV. Peak rating of DPV curves was retained for all processes occurring at the appropriate potentials of the other methods. The CV and DPV currents are directly proportional to the concentration. The linear dependence of the peak currents from CV and DPV depending on the P545 concentration is inserted in Figure 7.51 for all peaks present in DPV and for a1, c1, c2, c3 in CV. Their equations and their correlation coefficients are presented in Table 7.18, which contains the peaks with the best correlation coefficients for CV and DPV.

It can be noticed that the first anode peak (a1) and all the cadence peaks have good correlation coefficients for DPV. The other peaks have lower correlation coefficients. This behavior can be explained by parallel and irreversible chemical and electrochemical processes. The slope of peak a1 is high in both DPC and CV, this process being attributed to the formation of the cation radical.

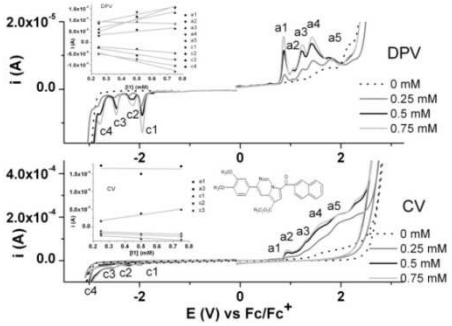

Figure 7.51. CV (0.1 Vs-1) and DPV (0.01 Vs-1) curves on glassy carbon electrode (diameter 3 mm) at different concentrations **P545** in 0.1M TBAP/CH_3CN; Inset Linear dependences of peak currents on concentration

Table 7.18. Equations and the correlation coefficients of peak currents linear dependences on concentration* for CV (0.1 Vs^{-1}) and DPV (0.01 Vs^{-1}) curves

Method	Equation*	Correlation coefficient
DPV	$i_{peak\ a1} = -0{,}82 \cdot 10^{-6} + 22{,}67 \cdot 10^{-6} \cdot$ [**P545**]	0,95636
	$i_{peak\ a3} = 2{,}87 \cdot 10^{-6} + 14{,}53 \cdot 10^{-6} \cdot$ [**P545**]	0,84782
	$i_{peak\ a4} = 5{,}50 \cdot 10^{-6} + 13{,}98 \cdot 10^{-6} \cdot$ [**P545**]	0,87285
	$i_{peak\ c1} = -0{,}65 \cdot 10^{-6} - 15{,}76 \cdot 10^{-6} \cdot$ [**P545**]	0,93869
	$i_{peak\ c2} = -4{,}89 \cdot 10^{-6} - 5{,}57 \cdot 10^{-6} \cdot$ [**P545**]	0,94141
	$i_{peak\ c3} = -0{,}075 \cdot 10^{-6} - 10{,}40 \cdot 10^{-6} \cdot$ [**P545**]	0,95433
	$i_{peak\ c4} = -2{,}39 \cdot 10^{-6} - 10{,}52 \cdot 10^{-6} \cdot$ [**P545**]	0,99556
CV	$i_{peak\ a1} = 1{,}999 \cdot 10^{-6} + 65{,}16 \cdot 10^{-6} \cdot$ [**P545**]	0,95169
	$i_{peak\ c2} = -14{,}11 \cdot 10^{-6} - 16{,}29 \cdot 10^{-6} \cdot$ [**P545**]	0,99976
	$i_{peak\ c3} = -18{,}32 \cdot 10^{-6} - 25{,}64 \cdot 10^{-6} \cdot$ [**P545**]	0,85887

* in the equations presented i is given in A, and [P545] in mmol /L (mM)

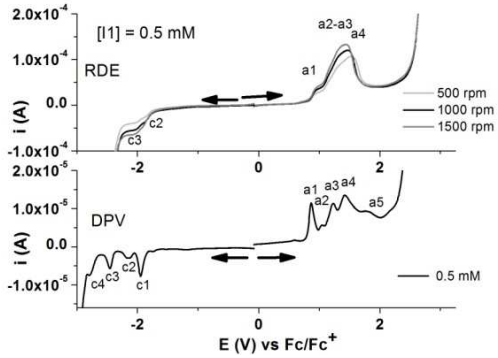

Figure 7.53. RDE curves on glassy carbon electrode at different rotation rates (500–1500 rpm) and DPV curves (0.01Vs^{-1}) obtained for **P545** in 0.1M TBAP/CH3CN

Figure 7.53 shows the anode and cathode RDE curves at different rotational speeds. To establish correspondence between the observed processes in the RDE curves and the pic processes observed in DPV, the anode and cathode RDE curves were put together with the DPV curve (for the same concentration). Cathode RDE curves obtained for P545 in 0.1 M TBAP CH3CN at different rotational speeds are normal. Globally, two anode peaks are observed, then the currents abruptly descend after reaching the potential of the a4 peak. The shape of the RDE curves confirms the electrode coating with an insulating layer in the anode potential range (at potentially more positive than a4).

Currents increase with the rotational speed of RDE. There is an isosbest point for the RDE curves at the potential of 1.547 V, which corresponds to a reversal of the current values obtained at different rotational speeds. Starting from this potential (corresponding to peak a4 in

DPV), the current becomes smaller to very small values and stays constant over a potential range of about 1 V.

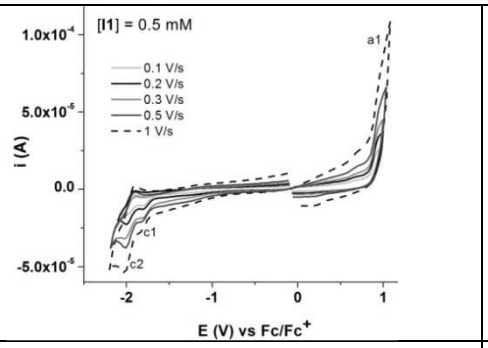

A

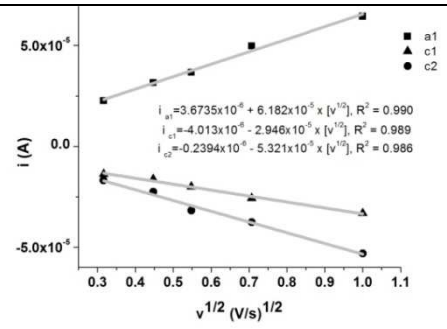

B

Figure 7.54. CV curves in 0.1M TBAP/CH3CN on glassy carbon electrode (3 mm diameter)for P1 (0.5 mM) at different scan rates (0.1 – 1 Vs-1) (A) and dependences of the peak currents on the square root of the scan rate (B)

To study the reversibility of the processes, CV curves were recorded at different scanning rates (0.1 - 1 Vs-1) for the first anodic peak a1 and the first cathodic peak c1 (Figure 7.54). Cathode drops have become more apparent with increasing of scanning rate. The linear dependence of the peak currents on the square root of the scanning rate is obtained for a1, c1 and c2 with the slopes given in Figure 7.54B.

Figure 7.55 shows the CV curves (0.1 Vs-1) obtained on different potential domains. Anodic processes are irreversible, while cathodic processes are mainly quasi-reversible (Table 7.19) [349].

Table 7.19. Peak potential values (V) vs Fc/Fc^+ for **P1** from DPV and CV curves

Pic	Metoda		Procesul asociat*
	DPV	CV	
a1	0,867	0,931	ireversibil
a2	1,044	-	ireversibil
a3	1,226	1,293	ireversibil
a4	1,418	1,587	-
a5	1,829	1,943	-
c1	-1,947	-1,992	cvasi reversibil
c2	-2,144	-2,207	cvasi reversibil
c3	-2,456	-2,518	cvasi reversibil
c4	-2,794	-	-

7.1.9. Electrochemical characterization for ethyl 3- (3,4-dimethoxyphenyl) -7- (2,4-dimethoxybenzoyl) pyrrolo [1,2- c] pyrimidine-5-carboxylate (P552)

Figure 7.56 shows the structure of pyrrolopyrimidine (**P552**).

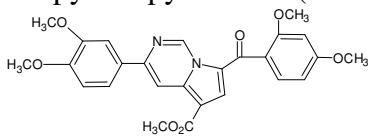

Figura 7.56. Structura aza-pirolopirimidinei **552**

The CV and DPV curves obtained at different concentrations of P552 (0 - 0.75 mM) are shown in Figure 7.57. The DPV curves at different concentrations have six anode peaks labeled with a1 - a6 and three cathode peaks (c1 - c3), in order of their occurrence in voltamograms. Curves CV have five anodic processes corresponding to DPV peaks (a1 - a5) and four cathodic processes indicated in relation to DPV cathode peaks (c1 - c4).

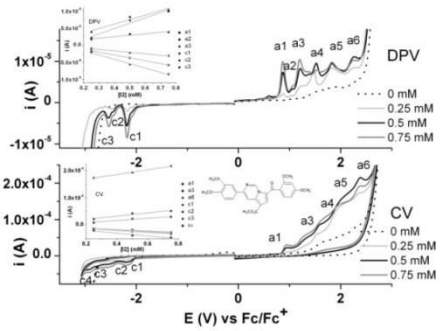

Figure 7.57. CV (0.1 Vs^{-1}) and DPV (0.01 Vs^{-1}) curves on glassy carbon electrode (diameter 3 mm) at different concentrations **P552**in 0.1M TBAP/CH_3CN; Inset Linear dependences of peak currents on concentration

Currents grow with concentration. The linear dependencies of the main peak currents for the CV and DPV curves are presented. The equations of the main currents of the pic according to the concentration of P552 and their correlation coefficients are presented in Table 7.21. The slopes obtained for P552 dependencies (Table 7.20) are lower than those for P545 (Table 7.19). This can be explained by a steric hindrance of the two methoxy groups in P552 and is not correlated with their molecular masses (MP545 <MP552).

Table 7.20. E Equations and the correlation coefficients of peak currents linear dependences on concentration* for CV (0.1 Vs^{-1}) and DPV (0.01 Vs^{-1}) curves

Metoda	Ecuația*	Coeficient de corelație
DPV	$i_{peak\ a1} = -1{,}38 \cdot 10^{-6} + 15{,}69 \cdot 10^{-6} \cdot$ [**P552**]	0,92769
	$i_{peak\ a2} = 0{,}82 \cdot 10^{-6} + 4{,}24 \cdot 10^{-6} \cdot$ [**P552**]	0,90322
	$i_{peak\ a3} = 0{,}96 \cdot 10^{-6} + 13{,}13 \cdot 10^{-6} \cdot$ [**P552**]	0,92993
	$i_{peak\ c1} = 0{,}99 \cdot 10^{-6} - 12{,}80 \cdot 10^{-6} \cdot$ [**P552**]	0,99393
	$i_{peak\ c2} = -0{,}04 \cdot 10^{-6} - 4{,}26 \cdot 10^{-6} \cdot$ [**P552**]	0,97888
	$i_{peak\ c3} = 0{,}5 \cdot 10^{-6} - 8{,}43 \cdot 10^{-6} \cdot$ [**P552**]	0,99988
CV	$i_{peak\ a1} = -0{,}03 \cdot 10^{-6} + 41{,}03 \cdot 10^{-6} \cdot$ [**P552**]	0,96173
	$i_{peak\ a3} = 9{,}02 \cdot 10^{-6} + 59{,}28 \cdot 10^{-6} \cdot$ [**P552**]	0,93475
	$i_{peak\ a6} = 150{,}48 \cdot 10^{-6} + 85{,}57 \cdot 10^{-6} \cdot$ [**P552**]	0,99441
	$i_{peak\ c1} = -6{,}88 \cdot 10^{-6} - 24{,}57 \cdot 10^{-6} \cdot$ [**P552**]	0,90949
	$i_{peak\ c2} = -6{,}39 \cdot 10^{-6} - 29{,}33 \cdot 10^{-6} \cdot$ [**P552**]	0,99953
	$i_{peak\ c3} = -5{,}83 \cdot 10^{-6} - 35{,}05 \cdot 10^{-6} \cdot$ [**P552**]	0,99994
	$i_{peak\ c3} = -9{,}02 \cdot 10^{-6} - 51{,}23 \cdot 10^{-6} \cdot$ [**P552**]	0,93303

* in the equations presented i is given in A, and [P545] in mmol /L (mM)

RDE curves at different rotational speeds (500-2000 rpm) for P545 are shown in Figure 7.58 compared to anodic and cathodic DPV curves. The RDE curves show two anode areas corresponding to the a1 and a5 peaks in DPV. Currents grow at the speed of rotation. After peak a5 the current drops sharply. This behavior is characteristic for coating the electrode with insulating films. The isosbest point (at about 2 V) is less marked for P552, compared to compound P545. Also, the passive field is much shorter (0.2 V) than for P545 (1 V). In the cathodic field, the waves are difficult to separate. These facts show that the film formed by P552 after the potential α5 is more porous than the one corresponding to P545.

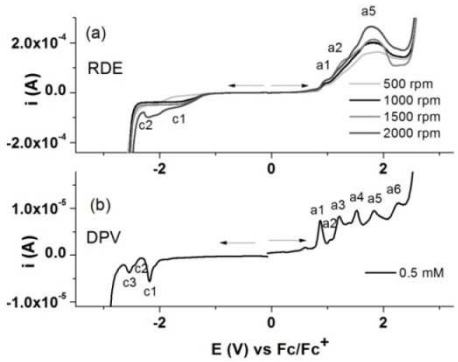

Figure 7.58. RDE curves on glassy carbon electrode at different rotation rates (500–1500 rpm) and DPV curves ($0.01Vs^{-1}$) obtained for **P552** in 0.1M TBAP/CH3CN

Figure 7.59 shows CV curves at different scanning speeds for P552 (0.5 mM) for peaks a1 and c1. With increasing scanning speed, a new anodic process (d) can be observed, having a corresponding process (d ') in the reverse sweep. Table 7.21 shows the equations and correlation coefficients for these peaks. It can be noticed that the currents are increasing at the speed of scanning. The absolute slope for α1 (~ 99 μA (V / s) -1/2) is approximately double the slope for c1 (~ 58 μA (V / s) -1/2) V / s) -1/2) D '(~ 11 μA (V / s) -1/2) are even lower. All these facts show that the pair d / d 'is due to a solvent impurity, while a1 and c1 can be attributed to P552 oxidation and reduction, also depend on P552 concentration. Their different slopes are due to a different number of electrons involved in the first peaks of oxidation and reduction.

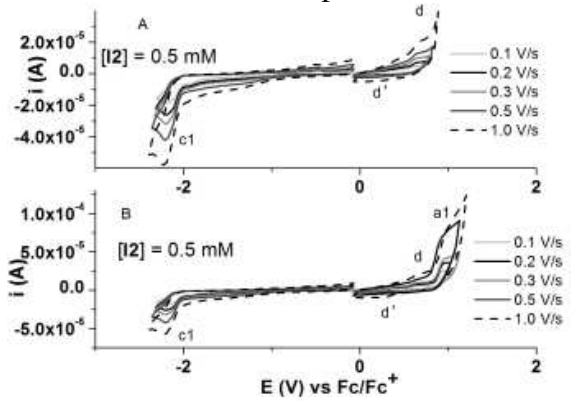

Figure 7.59. CV curves in 0.1M TBAP/CH_3CN on glassy carbon electrode (3 mm diameter) for **P552** (0.5 mM) at different scan rates ($0.1 – 1\ Vs^{-1}$)

Table 7.21. Equations and correlation coefficients for CV curves at different scan rates

Peak	Equation	Correlation coefficient
d	$i_{peak\ d} = -2{,}56 + 21{,}99 \cdot [\mathbf{v^{1/2}}]$	0,997
a1	$i_{peak\ a1} = -7{,}65 + 98{,}69 \cdot [\mathbf{v^{1/2}}]$	0,949
d’	$i_{peak\ d1'} = 2{,}42 - 11{,}29 \cdot [\mathbf{v^{1/2}}]$	0,941
c1	$i_{peak\ c1} = -0{,}38 - 57{,}68 \cdot [\mathbf{v^{1/2}}]$	0,998

*i_{peak} este exprimat in μA şi v este viteza de baleiaj (V/s)

CV curves for P552 in different domains (0.1 Vs-1) are shown in Figure 7.60 The processes associated with the curves and their characteristics are presented in Table 7.22. Cathodic poles are quasi-reverse [349].

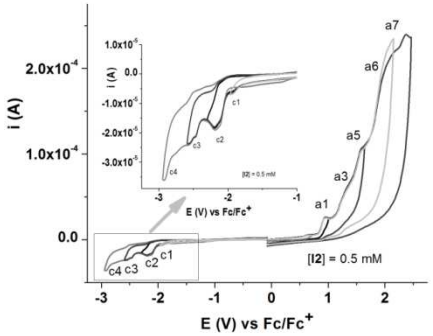

Figure 7.60. CV curves (0.1 Vs^{-1}) on glassy carbon electrode (3mm diameter)on different scan domains for **P552** (0.5 mM) in 0.1M TBAP/CH_3CN

Tabelul 7.22. Peak potentials values (V) vs $Fc/Fc^+$from DPV and CV curves for **P552**

Pic	Metoda		Procesul asociat*
	DPV	CV	
a1	0,87	0,94	ireversibil
a2	1,04	-	-
a3	1,21	1,26	ireversibil
a4	1,52	1,58	ireversibil
a5	1,83	1,97	cvasi reversibil
a6	2,26	2,38	ireversibil
c1	-2,18	-2,19	ireversibil
c2	-2,45	-2,47	ireversibil
c3	-2,55	-2,55	cvasi reversibil
c4	-	-2,91	cvasi reversibil

7.2. COMPARISONS BETWEEN ELECTROCHEMICAL BEHAVIORS OF PIROLOPYRIMIDES

Tables 7.33 and 7.34 show the potential of the anode and cathode peaks in the anodic and cathodic DPV and CV curves at the 0.5 mM concentration.

From Table 7.34 it can be seen that P417 is most rapidly oxidized, and compounds P565, P311 and P335 are reduced. Unless the first peak from P417 is taken into account, the P335, P338 and P543 compounds are first oxidized.

To calculate the diffusion coefficient the Randles-Sevcik equation with the formula $i_p = 268600 \cdot n^{3/2} \cdot A \cdot C \cdot D^{1/2} \cdot v^{1/2}$, where ip = the peak current in the ampoules, A = the area of the electrode in cm2, v = the velocity variation in V / s, D = the diffusion coefficient in Cm2 / s, C = concentration in mmol / L, n = number of transferred electrons. From the velocity influence on the anode domain the slope (ip vs v1 / 2) was determined after the first anodic peak and was replaced in the above formula. Table 7.35 lists the values obtained for calculating the diffusion coefficient.

To calculate the number of transferred electrons we need the slope of the slope from the anodic and right slope velocity obtained from the curve i (t) of the potentials are the peak peaks potential in the anodic and cathodic fields. Table 7.36 shows the values of n obtained for the anodic and cathodic field [331].

General strudture

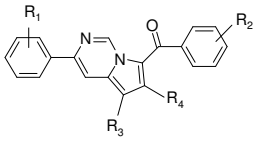

Compus	R1	R2	R3	R4
P311	3,4-diMeO	3-NO_2	CO_2Et	CO_2Et
P319	2-MeO	H	CO_2Me	CO_2Me
P335	3-MeO	3-NO_2	CO_2Et	CO_2Et
P338	2,4-diMeO	4-Br	CO_2Me	CO_2Me
P376	3,4-diMeO	4-F	CO_2Et	H
P417	3,4,5-triMeO	H	CO_2Me	CO_2Me
P543	3,4-diMeO	4-Me	CO_2Et	H
P545	545-P (**I10**)	3,4-diMeO	2-naftil *	CO_2Et
P552	552-P (**I11**)	3,4-diMeO	2,4-diMeO	CO_2Et
P557	557-P (**I12**)	2,4-diMeO	2-naftil *	CO_2Et
P563	2,4-diMeO	4Me	CO_2Et	H
P565	3-Me	3-NO_2	CO_2Me	CO_2Me
P585	3,4-diMeO	2,4-diMeO	CO_2Me	CO_2Me

* 2-naftil inlocuieste radicalul R1-fenil legat de nucleul pirolo[1,2-c]pirimidinic sau radicalul R2-fenil legat de C=O

Table 7.33. Anodic and cathodic peaks potential (V) for compound (DPV 0.5mM) vs. Fc/Fc^+

Comp / Pic DPV	**P311**	**P319**	**P335**	**P338**	**P376**	**P417**	**P543**	**P565**	**P585**
anodic	0,93 1,10 1,33	1,09 1,50 1,66 2,04	0,84 1,16 1,70 2,21	0,87 1,74 1,90	0,86 1,04 1,21 1,70 2,16	0,39 0,87 1,11 1,30 1,59 2,04	0,86 1,03 1,20 1,46 1,78	1,22 1,49 1,88	0,82 0,98 1,18 1,42 1,76 2,14
catodic	-1,39 -1,82 -2,02 -2,43 -2,88	-1,99 -2,37 -2,45 -2,65 -2,91	-1,42 -1,85 -2,02 -2,43 -2,79	-1,85 -2,00 -2,15 -2,43 -2,52 -2,88	-2,00 -2,21 -2,48 -2,78	-1,87 -2,28 -2,46 -2,55 -2,69	-2,03 -2,20 -2,44 -2,73	-1,38 -1,78 -1,98 -2,39 -2,78	-2,09 -2,15 -2,58 -2,97

Table 7.34. Anodic and cathodic peaks potential (V) for compound (CV 0.5mM) vs Fc/Fc^+

Comp / Pic CV	**P311**	**P319**	**P335**	**P338**	**P376**	**P417**	**P543**	**P565**	**P585**
anodic	1,0	1,13 1,62 1,91 2,12	1,22 1,84 2,35	0,91 1,79 2,32	0,92 1,26 1,85 2,20	0,44 0,94 2,41	0,91 1,27 1,92	1,29	0,95 1,31 1,58 1,93 2,34
catodic	-1,45 -1,88 -2,08 -2,46 -2,95	-2,02 -2,49 -2,67 -2,94	-1,43 -1,85 -2,05 -2,46 -2,83	-1,89 -2,02 -2,17 -2,44 -2,54 -2,81	-2,07 -2,34 -2,53 -2,88	-2,01 -2,34 -2,60 -2,87	-2,09 -2,28 -2,49 -2,87	-1,84 -2,07 -2,48 -2,85	-2,12 -2,55 -2,93

Tablel 7.35. Calculation of diffusion coefficients for 0.5 mM concentration

Compus	R1	R2	R3	R4	Panta dreptei	$10^5 \times D$ (cm^2/s)
P311	3,4-diMeO	3-NO_2	CO_2Et	CO_2Et	0,000096	10,20
P319	2-MeO	H	CO_2Me	CO_2Me	0,000177	34,66
P376	3,4-diMeO	4-F	CO_2Et	H	0,0000813	7,32
P417	3,4,5-triMeO	H	CO_2Me	CO_2Me	0,000023	0,59
P543	3,4-diMeO	4-Me	CO_2Et	H	0,000155	26,58
P565	3-Me	3-NO_2	CO_2Me	CO_2Me	0,000251	69,70
P585 (pic a1)	3,4-diMeO	2,4-diMeO	CO_2Me	CO_2Me	0,000031	1,06
P585 (pic a2)	3,4-diMeO	2,4-diMeO	CO_2Me	CO_2Me	0,000068	51,16

The results in table 7.36 are preliminary results to be analyzed and interpolated because they are not consistent with the expected results. By comparing the data from column 2 to 3, if the two methods give comparable results, the assessment based on the cathodic slope of the number of transferred electrons is more correct, we will compare 4 to 7 and we find that they do not fit; in the cathodic field the benzoyl group is reduced (The reduction has 2 electrons).

Figure 7.88 shows the anodic and cathode chronoamperometric curves and the linear dependencies of the anodic and cathodic currents depending on the time difference.

CHAPTER 8
OBTAINING ELECTRODES MODIFIED WITH INDOLISINE

Vitrified carbon electrodes modified with poly (indolizine) polyol films (at a concentration of 0.5 mM) were obtained in millimolar solution using 0,1 M TBAP / CH3CN support electrolyte by successive sweep or by potentially controlled electrolysis (CPE) To different tasks or potentials. The modified electrodes were transferred to a cell containing 1 mM ferrocene in 0.1 M TBAP / CH3 CN. All potentials were corrected with the ferrocene / ferricin couple potential (Fc / Fc +) which, under our experimental conditions, was 0.07 V.

8.8. ELECTRODES MODIFIED BASED ON **P545**

The modified polyP545 electrodes were prepared in the 0.5 mM solution of P545 in 0.1 M TBAP, CH3 CN by successive successive -0.3 V potential bends and various anode boundaries (Figure 8.15). The modified electrodes were transferred to ferrocene solution (1 mM) in 0.1 M TBAP / CH3CN and the CV curves were recorded and compared with the ferrocene signal on the naked electrode (Figure 8.15f). The modified electrode ferrocene signal prepared by successive sweep with a potential limit of up to 2.02 V is much lower than for other limits. This shows that electrode coverage is more efficient at this potential due to the processes taking place at this potential. The resulting film covers the electrode much better.

Modified electrodes were also prepared by potentially controlled electrolysis (CPE). Figure 8.16a shows the comparison of CV curves for modified electrodes prepared by CPE at different potentials and constant loads. In Figure 8.16b it is observed that for the 2 mC films the ferrocene current is constant for both the anode peaks (ipa) and the cathode peaks (ipc) (Figure 8.16b). However, at the higher applied potentials (2.35 V) there is a significant decrease in the anode and cathodic potential of ferrocene (Epa and Epc) and also in the formal potential (Ef) (Figure 8.16c) .

For CPE, loads greater than 4 mC and 6 mC were used to check the growth of the film. Figure 8.16d, 8.16e (Figure 8.16 f). The ferrocene signal for modified electrodes obtained at 2 mC for all anode potentials is close to that of the uncovered electrode (Figure 8.16b); This indicates the formation of a thin conductive film. For loads higher than 4 and 6 mC, the ferrocene signal is lower, indicating that thicker films are formed. Because the load is higher (6 mC), the decrease is more pronounced. The duration of the potential pulse is also important in film

formation (Table 8.1). It can be seen that for CPE of 6 mC to 2.02 V the pulse lasts longer (371 s) than the pulse at 2.35 V (66 s). Therefore, the best coating of the electrode was obtained at 2.02 V for a load of 6 mC, when the time for forming the film is higher [349].

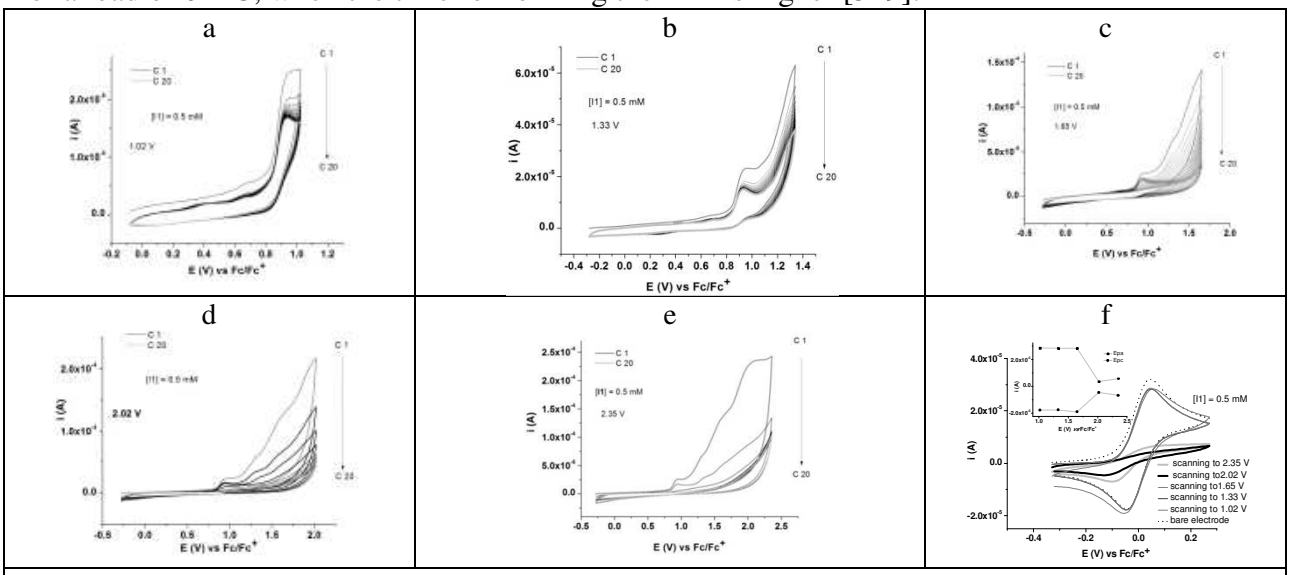

Figure 8.15. CV curves (0.1 Vs-1) during the preparation of the chemically modified electrode by successive scans in 0.5mM solution of **P545** in 0.1M TBAP, CH_3CN between -0.3 V and different anodic limits: 1.02 V (a), 1.33 V (b), 1.65 V (c), 2.02 V (d), 2.35 V (e) and CV curves (0.1V/s) for CME prepared by successive scans after the transfer of CME in 1mM ferrocene solution in 0.1 MTBAP, CH_3CN (f);

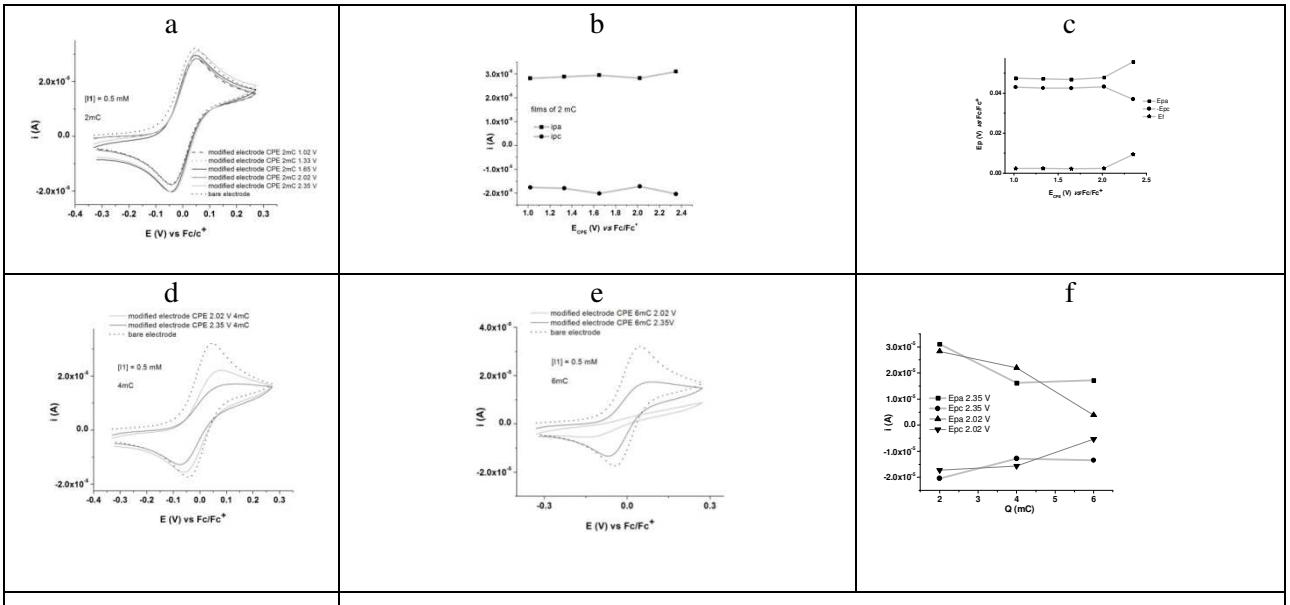

Figura 8.16. Curbe CV (0.1 Vs^{-1}) in 1 mM soluţie de ferocen in 0.1M TBAP, CH_3CN pe electrozi modificaţi preparaţi prin CPE in 0.5 mM solution of **P545** in 0.1M TBAP, CH_3CN la 2 mC (a), 4 mC (d) şi 6 mC (e) folosind diferite potenţiale de electropolimerizare; dependenţele picurilor/curenţilor anodici vs potenţialul de electropolimerizare (b)/(c) şi curentul ferocenului vs sarcina de electropolimerizare (f)

Table 8.1. CPE duration at different potentials (V) and charges (mC)

Potenţial CPE	Durata pulsului	Potenţial CPE	Durata pulsului	Potenţial CPE	Durata pulsului
(V)	(s)	(V)	(s)	(V)	(s)
2 mC		4 mC		6 mC	
2.35	3.2	2.35	32	2.35	66
2.02	12	2.02	90	2.02	371
1.65	30.4	-	-	-	-
1.33	85	-	-		-
1.02	332	-	-	-	-

8.9. ELECTRODES MODIFIED BASED ON **P552**

The preparation of P552-modified electrodes was done in a similar way as for P545 by successive cycles (Figure 8.17), or by CPE at different anode potentials or loads (Figure 8.18). Modified electrode ferrocene signals obtained at 6 mC and 8 mC are diminished. The decrease is more significant at 2.14 V because the pulse time is higher and there is more time for polymer formation (Table 8.2), as in the case of P545. Modified electrodes with charges of 0,3 mC, 0,8 mC, 1 mC and 1,1 mC are not covered by films [349]

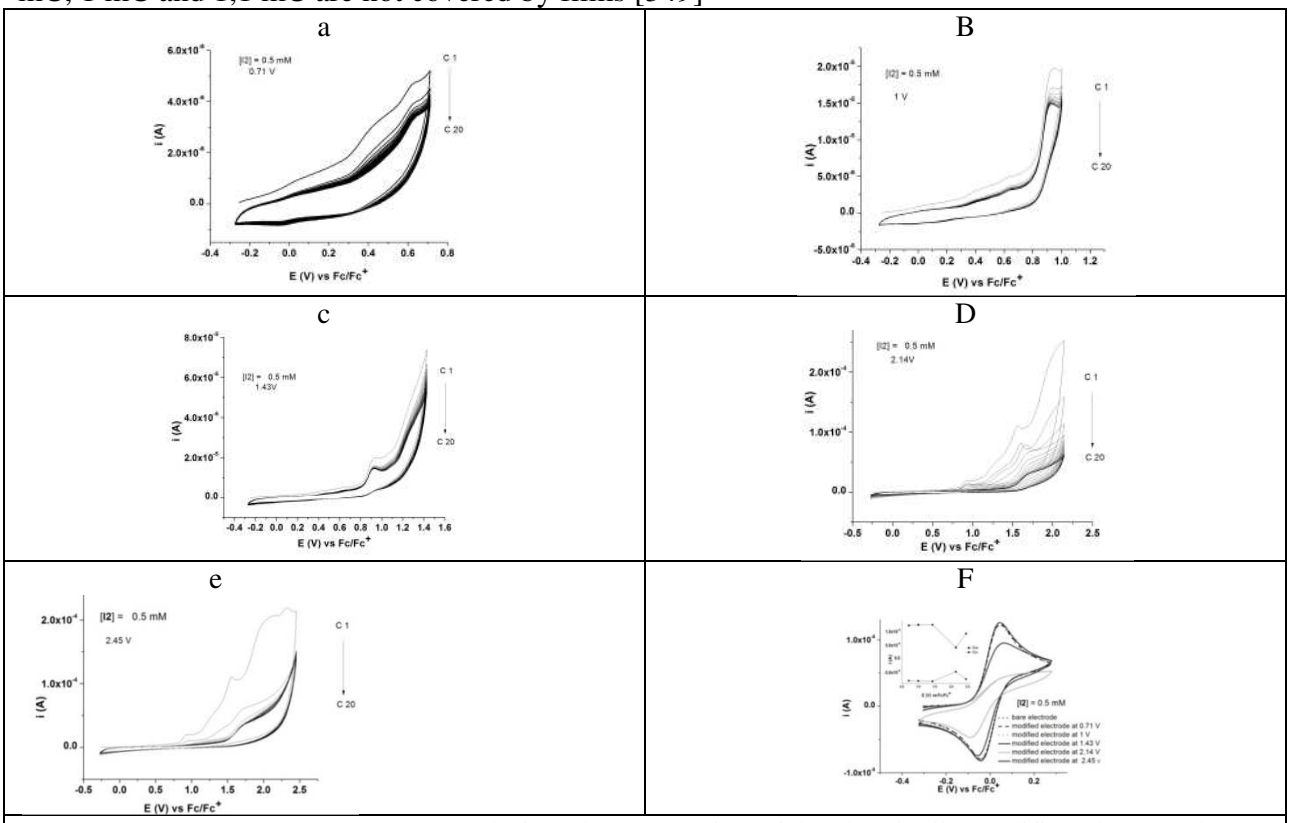

Figura 8.17. CV curves (0.1 Vs-1) during the preparation of the chemically modified electrode by successive scans in 0.5mM solution of **P552** in 0.1M TBAP, CH_3CN between -0.3 V and different anodic limits: +0.71 V (a), +1 V (b), +1.43 V (c), +2.14 V (d), 2.45 V (e) and CV curves (0.1V/s) for CME prepared by successive scans after the transfer of CME in 1mM ferrocene solution in 0.1 MTBAP, CH_3CN (f)

Table 8.2 CPE duration at different potentials (V) and charges (mC)

Sarcina	Durata pulsului	Sarcina	Durata pulsului
mC	sec	mC	sec
2.14 V		2.45 V	
0.8	8.3	-	-
1.1	10	1.1	8.3
2	16.4	-	-
3	31.7	-	-
4	43.5	4	30.4
6	107.7	6	46.3
8	152.1	-	-

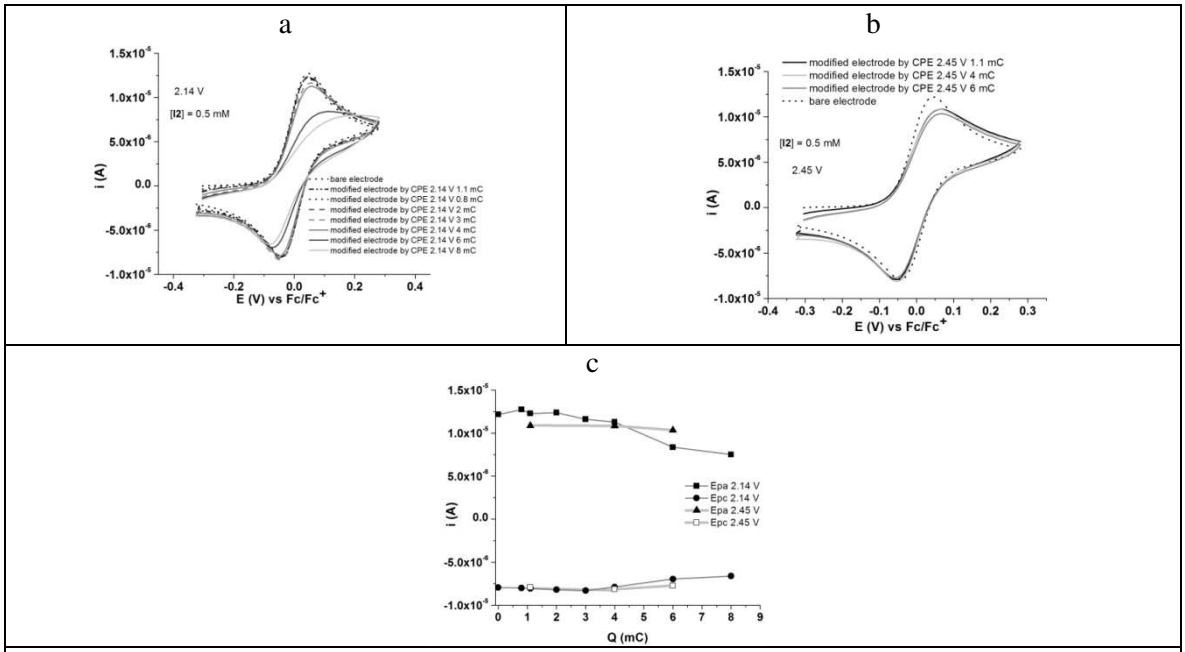

Figure 8.18. CV curves (0.1V/s) for CME based on **P552** (0,5 mM) in ferocen solution 1 mM in 0.1M TBAP, CH_3CN at 2.14 V (a) şi +2.45 V (b) using different electopolimerization charges; linear dependence currents vs charges (c)

8.14 COMPARISON BETWEEN ELECTRODES MODIFIED WITH POLIPIROLOPIRIMIDINE

8.14.1. Comparison between modified electrodes based on of polyP545 and polyP552

There are several differences in the preparation of modified electrodes prepared from P545 and P552 (Figure 8.27) either by CPE or by cycling. It can be seen that the transfer of modified electrodes (in 1 mM ferrocene solution) obtained by CPE at the same load (6 mC) and near potential (2.02 V for compound P545 and 2.14 V for compound P552), the ferrocene signal is flatter for P545 , Indicating a less conductive film (Figure 8.27a). The electrode appears to be better covered for P545 than P552. However, when the films are prepared by cycling, the differences are less significant (Figure 8.27b). This behavior can be explained by the fact that the preparation of the modified electrodes lasts longer through cycling (than by CPE) for both P545 and P552, and the polymerization stage can be better [349].

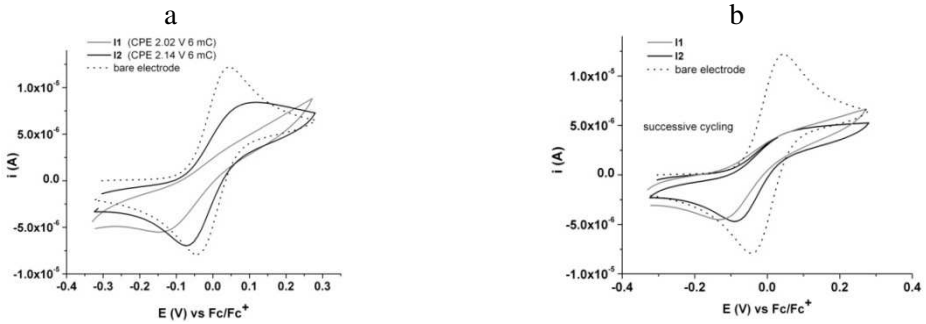

Figure 8.27. CV curves (0.1V/s) for CME based on **P545** (0,5 mM) and **P552** (0,5 mM) in ferocen solution 1mM in 0.1M TBAP, CH_3CN: by CPE (a), by succesiv scaning (b)

1. CONCLUSIONS

C.1. GENERAL CONCLUSIONS

22 new pyrrolo[1,2-c]pyrimidine derivatives have been synthesized: *3-(4-biphenylyl)-5-acetyl-7-(4-chlorobenzoyl)pyrrolo[1,2-c]pyrimidine* (**4a**), *3-(4-biphenylyl)-5-acetyl-7-(3-nitrobenzoyl)pyrrolo[1,2-c]pyrimidine* (**4b**), *ethyl 3-(4-biphenylyl)-7-(4-fluorobenzoyl)pyrrolo[1,2-c]pyrimidine-5-carboxylate* (**4c**), *ethyl 3-(4-biphenylyl)-7-(4-bromobenzoyl)pyrrolo[1,2-c]pyrimidine-5-carboxylate* (**4d**), *ethyl 3-(4-biphenylyl)-7-(4-nitrobenzoyl)pyrrolo[1,2-c]pyrimidine-5-carboxylate* (**4e**), *ethyl 3-(4-biphenylyl)-7-(3,4-dimethoxybenzoyl)pyrrolo[1,2-c]pyrimidine-5-carboxylate* (**4f**), d*imethyl 3-(4-biphenylyl)-7-(4-nitrobenzoyl)pyrrolo[1,2-c]pyrimidine-5,6-dicarboxylate* (**4g**), *diethyl 3-(4-biphenylyl)-7-(4-phenylbenzoyl)pyrrolo[1,2-c]pyrimidine-5,6-dicarboxylate* (**4h**), *diethyl 3-(4-biphenylyl)-7-(2-naphthoyl)pyrrolo[1,2-c]pyrimidine-5,6-dicarboxylate* (**4i**), *3-(4- biphenylyl)-5-acetil-7-(4-nitrobenzoyl) pyrrolo[1,2-c]pyrimidine* (**4j**), *dimethyl 3-(2-methoxyphenyl)-7-benzoyl-pyrrolo[1,2-c]pyrimidine-5,6-dicarboxylate* (**P319**), *diethyl 3-(3-methoxyphenyl)-7-(3-nitrobenzoyl)pyrrolo[1,2-c]pyrimidine-5,6-carboxylate* (**P335**), *dimethyl 3-(2,4-dimethoxyphenyl)-7-(4-bromobenzoyl)pyrrolo[1,2-c]pyrimidine-5,6-dicarboxylate* (**P338**), *ethyl 3-(2,4- dimethoxyphenyl)-7-(2,4- dimethoxybenzoyl) pyrrolo[1,2-c]pyrimidine-5-carboxylate* (**P557**), *ethyl 3-(2,4-dimethoxyphenyl)-7-(4-methylbenzoyl)pyrrolo[1,2-c]pyrimidine-5-carboxylate* (**P563**), *ethyl 3-(3,4-dimethoxylphenyl)-7-(4-fluorobenzoyl)pyrrolo[1,2-c]pyrimidine-5-carboxylate* (**P376**), *ethyl 3-(3,4-dimethoxylphenyl)-7-(4-methylbenzoyl)pyrrolo[1,2-c]pyrimidine-5-carboxylate* (**P543**), d*iethyl 3-(3,4-dimethoxylphenyl)-7-(3-nitrobenzoyl)pyrrolo[1,2-c]pyrimidine-5,6-dicarboxylate* (**P311**), *ethyl 3-(3,4-dimethoxylphenyl)-7-(2,4-dimethoxybenzoyl)pyrrolo[1,2-c]pyrimidine-5-carboxylate* (**P552**), *ethyl 3-(3,4-dimethoxyphenyl)-7-(2,naphtyl)pyrrolo[1,2-c]pyrimidine-5-carboxylate* (**P545**), *dimethyl 3-(3,4,5- trimethoxylphenyl)-7- pyrrolo[1,2-c]pyrimidine -5,6-di carboxylate* (**P417**), *dimethyl 3-(3-methylphenyl)-7-(3-nitrobenzoyl)pyrrolo[1,2-c]pyrimidine-5,6-dicarboxylate* (**P565**) in order to obtain compounds that can be used for sensors.

For the synthesis of these compounds the one pot three components method was used. For the identification of the structures of the compounds obtained, mass spectrometry, IR, 1 H-NMR and 13 C-NMR was used.

The luminescent properties of all compounds were determined by absorption spectroscopy and fluorescence. Specific parameters such as extinction coefficient, Stokes displacement, quantum yield, and Stern-Volmer constant (KSV) were calculated. For the 3-phenylpyrrolo [1,2-c] pyrimidine derivatives, influence of the polarity of the solvents on the absorption and emission spectra was studied. From these studies, it can be seen that the polarity of the solvent influences

the shape of the spectrum, the absorption and emission wavelength, and the absorbance and fluorescence intensity of the compound.

The compounds 319-P, 335-P, 338-P, 557-P, 563-P, 376-P, 543-P, 311-P, 552-P, 545-P, 417-P, 565-P Electrochemically characterized by cyclic voltammetry, differential pulse voltammetry and rotating disc electrodes. Specific anode and cathode processes have been identified. Modified pyrrolopyrimidine electrodes were obtained by successive cycles and by potentially controlled electrolysis. The modified pyrrolopyrimidine electrodes were transferred to the ferrocene to verify that a film was formed on the surface of the electrode.

C.2. ORIGINAL CONTRIBUTIONS

22 new pyrrolo[1,2-c]pyrimidine derivatives have been synthesized: *3-(4-biphenylyl)-5-acetyl-7-(4-chlorobenzoyl)pyrrolo[1,2-c]pyrimidine* (**4a**), *3-(4-biphenylyl)-5-acetyl-7-(3-nitrobenzoyl)pyrrolo[1,2-c]pyrimidine* (**4b**), *ethyl 3-(4-biphenylyl)-7-(4-fluorobenzoyl)pyrrolo[1,2-c]pyrimidine-5-carboxylate* (**4c**), *ethyl 3-(4-biphenylyl)-7-(4-bromobenzoyl)pyrrolo[1,2-c]pyrimidine-5-carboxylate* (**4d**), *ethyl 3-(4-biphenylyl)-7-(4-nitrobenzoyl)pyrrolo[1,2-c]pyrimidine-5-carboxylate* (**4e**), *ethyl 3-(4-biphenylyl)-7-(3,4-dimethoxybenzoyl)pyrrolo[1,2-c]pyrimidine-5-carboxylate* (**4f**), d*imethyl 3-(4-biphenylyl)-7-(4-nitrobenzoyl)pyrrolo[1,2-c]pyrimidine-5,6-dicarboxylate* (**4g**), *diethyl 3-(4-biphenylyl)-7-(4-phenylbenzoyl)pyrrolo[1,2-c]pyrimidine-5,6-dicarboxylate* (**4h**), *diethyl 3-(4-biphenylyl)-7-(2-naphthoyl)pyrrolo[1,2-c]pyrimidine-5,6-dicarboxylate* (**4i**), *3-(4- biphenylyl)-5-acetil-7-(4-nitrobenzoyl) pyrrolo[1,2-c]pyrimidine* (**4j**), *dimethyl 3-(2-methoxyphenyl)-7-benzoyl-pyrrolo[1,2-c]pyrimidine-5,6-dicarboxylate* (**P319**), *diethyl 3-(3-methoxyphenyl)-7-(3-nitrobenzoyl)pyrrolo[1,2-c]pyrimidine-5,6-carboxylate* (**P335**), *dimethyl 3-(2,4-dimethoxyphenyl)-7-(4-bromobenzoyl)pyrrolo[1,2-c]pyrimidine-5,6-dicarboxylate* (**P338**), *ethyl 3-(2,4- dimethoxyphenyl)-7-(2,4- dimethoxybenzoyl) pyrrolo[1,2-c]pyrimidine-5-carboxylate* (**P557**), *ethyl 3-(2,4-dimethoxyphenyl)-7-(4-methylbenzoyl)pyrrolo[1,2-c]pyrimidine-5-carboxylate* (**P563**), *ethyl 3-(3,4-dimethoxylphenyl)-7-(4-fluorobenzoyl)pyrrolo[1,2-c]pyrimidine-5-carboxylate* (**P376**), *ethyl 3-(3,4-dimethoxylphenyl)-7-(4-methylbenzoyl)pyrrolo[1,2-c]pyrimidine-5-carboxylate* (**P543**), d*iethyl 3-(3,4-dimethoxylphenyl)-7-(3-nitrobenzoyl)pyrrolo[1,2-c]pyrimidine-5,6-dicarboxylate* (**P311**), *ethyl 3-(3,4-dimethoxylphenyl)-7-(2,4-dimethoxybenzoyl)pyrrolo[1,2-c]pyrimidine-5-carboxylate* (**P552**), *ethyl 3-(3,4-dimethoxyphenyl)-7-(2,naphtyl)pyrrolo[1,2-c]pyrimidine-5-carboxylate* (**P545**), *dimethyl 3-(3,4,5- trimethoxylphenyl)-7- pyrrolo[1,2-c]pyrimidine -5,6-di carboxylate* (**P417**), *dimethyl 3-(3-methylphenyl)-7-(3-nitrobenzoyl)pyrrolo[1,2-c]pyrimidine-5,6-dicarboxylate* (**P565**). The new 3-biphenylpyrrolo [1,2-c] pyrimidine derivatives were synthesized by a 1,3-dipolar cycloaddition of pyrimidinium-N-amides with deficient electrons, using the one three components component which is presented in the literature .

The fluorescent properties of this class of compounds have been investigated for the first time. Their absorption and emission spectra were recorded in acetonitrile: chloroform (1: 1) and their main spectral characteristics were evaluated: Stokes displacement, quantum yield and fluorescence extinction. The effect of the structure on the fluorescent properties was investigated. It has been shown that the benzene ring at the 3-position or the benzoyl group at the 7-position strongly influence the fluorescence of the compounds in the blue-green region of the visible spectrum. Substituents on the phenyl and benzoyl moieties have a greater contribution to the fluorescence of pyrrolo [1,2-c] pyrimidines. The highest value of quantum yield for 3-biphenylpyrrolopyrimidine derivatives was obtained for ethyl 3- (4-biphenyl) -7- (3,4-dimethoxybenzoyl) pyrrolo [1,2- c] pyrimidine-5-). In the case of 3-phenylpyrrolopyrimidine derivatives the highest quantum yield was obtained for compound 8 ethyl 3- (3,4-

dimethoxyphenyl) -7- (4-methylbenzoyl) pyrrolo [1,2- c] pyrimidine-5-carboxylate 543-P), 61.35% in chloroform 22.90% in methylene chloride, 52.6% in acetonitrile, 87.25% in DMSO

The effect of the solvent on the absorption and fluorescence spectra of the investigated compounds was studied. Absorption and fluorescence spectra of 3-12 pyrrolopyrimidines were recorded in increasing polarity solvents: chloroform, dichloromethane, acetonitrile and dimethylsulfoxide. The correlation between the solvent parameters and the absorption-emission properties of compounds **3-12** was investigated by the Lippert-Mataga and Kawski-Chamma-Viallet methods to calculate the dipole moments of the compounds in the basal states and excited by the multiple linear regression method Kamlet- Taft. It has been shown that the polarity of the solvents is the most important parameter that influences the emission spectra. It has been shown that the solvent aspect is very complex and strongly depends on the nature of the substituents. This phenomenon is caused by the difference in conjugation or migration of the non-participating electron pairs.

Subsequent studies to determine the electrochemical properties of all these compounds are welcome, given their direct relevance for finding practical applications of these sensor compounds.

C3. OUTLOOK

The doctoral thesis elaborated opens new perspectives related to:

• Synthesis of new pirolo [1,2-c] pyrimidine derivatives as a structure of compounds that can be used to produce OLEDs or solar cells.

• Establish electrochemical and spectral properties for other compounds in this class that have not been used in this study.

• Determining the fluorescence lifetime of the studied compounds in order to see if they can be used to obtain advanced fluorescence materials

• Dissemination of unplanned experimental results

• Use of modified pyrrolo-pyrimidine electrodes as sensors for metal detection.

APPENDICES

List of contributions elaborated during this thesis

Papers

1. **M.-L. Tatu**, E. Georgescu, C. Boscornea, M. M. Popa, E. M. Ungureanu, *Synthesis and spectral characterization of 1-[7-(4-nitrobenzoyl)-3-(biphenyl-4 yl)pyrrolo[1,2-c]pyrimidin-5-yl]ethanone*, Scientific Bulletin, Series B, Chemistry and Materials Science, Vol. 77, Iss. 3, pp. 49-58, 2015. **IF**: -; **SRI**: -.
2. **M.-L. Tatu**, E. Georgescu, C. Boscornea, M. M. Popa, E. M. Ungureanu, *Synthesis and fluorescence of new 3-biphenylpyrrolo[1,2-c]pyrimidines*, Arabian Journal of Chemistry, Vol. 10, Iss. 5, pp. 643-652, 2017. **IF**: **4,553**; **SRI**: **2,406**.
3. **M.-L. Tatu**, F. Harja, E.-M. Ungureanu, E. Georgescu, M.-M. Popa, *Electrochemical Characterization of Some Pyrrolo[1,2-c]Pyrimidine Derivatives*, Revista de Chimie, acceptat (publicat in vol 2/2018). **IF**: **1.232**; **SRI**: **0,164**
4. **M.-L. Tatu**, E. Georgescu, C. Boscornea, M. M. Popa, G. Stanciu, E. M. Ungureanu, *A comparative study on the fluorescence of several pyrrolo[1,2-c]pyrimidines*, Arabian Journal of Chemistry, submitted.
5. **M.-L. Tatu**, F. Harja, E.-M. Ungureanu, E. Georgescu, L. Birzan, M.-M. Popa, *Electrochemical studies of two pyrrolo[1,2-c]pyrimidines*, Bulgarian Chemical Communication, (accepted) **IF: 0,238, SRI: 0,181**
   FIC: 6,023; SRI cumulat: 2,751

Conferences

1. M. L. Tatu, E. Georgescu, C. Boscornea, M.M. Popa, E.-M. Ungureanu, *Syntesis* and *fluorescence of new 3- biphenylpyrrolo[1,2-c]pirimidines*, International symposium, Priorities of Chemistry for a Sustainable Development, PRIOCHEM, XI edition, Bucharest, October 29 – 30, 2015.
2. M. L. Tatu, E. Georgescu, C. Boscornea, M. M. Popa, E. M. Ungureanu, *Electrochemical characterization of some biphenylpyrrolo[1,2-c]pirimidines derivates*, Symposium of the Young Chemical Engineers, SICHEM 2016,8 – 9 Septembrie 2016, Bucharest.
3. M. L. Tatu, E. Georgescu, C. Boscornea, M. M. Popa, E. M. Ungureanu, *Propriétés d'absorption, de fluorescence et électrochimiques de plusieurs[1,2-c]pyrimidines*, NOMAREES 2016, 28 – 31 August, Iasi. (de completat conferinta numarul)
4. M. L. Tatu, E. Georgescu, C. Boscornea, M. M. Popa, E. M. Ungureanu, *Syntesis of new 3-phenylpyrrolo[1,2-c]pirimidines*, International Symposium „Mediul şi Industria (Enviroment and Industry)" – SIMI 2016, Octomber 13-14, Bucharest.
5. E. A. Matei, M. C. Craciun, C. Iacobescu, I. Marasescu, Facultatea CASM, coordonatori stiintifici E.M. Ungureanu, M. L. Tatu, *Studii de fluorescență asupre unor compusi organici*, – prezentare orală la Sesiunea de Comunicări Științifice Studențești 2014, mai 2014, Polizu - Universitatea POLITEHNICA din București
6. A. M. M. Dilimoț, Facultatea CASM, E.M. Ungureanu, M. L. Tatu, *Studii de fluorescență a unor compuși organici*,– prezentare orală Sesiunea de Comunicări Științifice Studențești 2015, mai 2015, Polizu – Unuversitatea POLITEHNICA din București, Romania.
7. I. Dumitru, G. Ionescu, Facultatea CASM, E.M. Ungureanu, M. L. Tatu, *Studii electrochimice în clasa indolizinelor* – prezentare orală Sesiunea de Comunicări Științifice Studențești 2016, mai 2016, Polizu – Unuversitatea POLITEHNICA din București, Romania.

The present summary contains in a concise form the content of chapters 4-8 of original contributions. The numbering of chapters, subchapters and tables corresponds to the one in the thesis. The bibliographic references used in the paper are presented.

Selective Bibliography:

[1]. *M. L. Tatu, E. Georgescu, C. Boscornea, M. M. Popa, E. M. Ungureanu*, "Synthesis and fluorescence of new 3-biphenylpyrrolo[1,2-c]pyrimidines", Arabian Journal of Chemistry, vol. **10**, Iss. 5, 2016, pp. 643-652.

[2]. *M. L. Tatu, E. Georgescu, C. Boscornea, M. M.l Popa, E. M. Ungureanu*, "Synthesis and spectral characterization of 1-[7-(4-nitrobenzoyl)-3-(biphenyl-4 yl)pyrrolo[1,2-c]pyrimidin-5-yl]ethanone", Scientific Bulletin, Series B, Chemistry and Materials Science, Vol. **77**, Iss. 3, 2015, pp 49-58.

[3]. *M .L. Tatu, F. Harja, E. M. Ungureanu, E. Georgescu, M. M. Popa,* Electrochemical Characterization of Some Pyrrolo[1,2-c]Pyrimidine Derivatives, Revista de Chimie, acceptat (publicat in vol 2/2018).

[4]. *M.-L. Tatu, E. Georgescu, C. Boscornea, M. M. Popa, G. Stanciu, E. M. Ungureanu,* A comparative study on the fluorescence of several pyrrolo[1,2-c]pyrimidines, Arabian Journal of Chemistry, submitted.

[5]. *M.-L. Tatu, F. Harja, E.-M. Ungureanu, E. Georgescu, L. Birzan, M.-M. Popa*, Electrochemical studies of two pyrrolo[1,2-c]pyrimidines, Bulgarian Chemical Communication, acceptat

[10]. *D. Chen, S. J. Su, Y. Cao*, "Nitrogen heterocycle-containing materials for highly efficient phosphorescent OLED swithlow operating voltage", J. Mater. Chem. C 2, 2014, pp 9565-9578.

[11]. *A. Buckley*, Organic Light-Emitting Diodes (OLEDs): Materials, devices and applications, Woodhead-Publishing, Cambridge UK, 2013.

[12]. *S. Oh, H. K. Lee, K. Y. Kim, S. S. Yoon*, "Highly efficient blue OLEDs based on diphenylaminofluorenylstyrenes end-capped with heterocyclic aromatics", Mat. Res. Bull. **47**, 2012, pp 2792-2795.

[13]. *A. Rotaru, I. Druta, E. Avram, R. Danac*,"Synthesis and properties of fluorescent 1,3-substituted mono and biindolizines", Arkivoc (**xiii**), 2009, pp 287-299.

[14].*A. Vlahovici, I. Druta, M. Andrei, M. Cotlet, R. Dinica*, "Photophysics of some indolizines, derivatives from bipyridyl, in various media", J. Luminesc. **82**, 1999, pp 155-162.
[15].*F. Dumitrascu, M. Vasilescu, C. Draghici, M. T. Caproiu, L. Barbu, D. G. Dumitrescu*, "New fluorescent indolizines and bisindolizinylethylenes", Arkivoc (**x**), 2011, pp 338-350.
[16].*G. N. Zbancioc, I. I. Mangalagiu*, "Microwave-assistedsynthesis of highly fluorescent pyrrolopyridazine derivatives", Synlett, 2006, pp 804-806.
[17]. *M. Vasilescu, R. Bandula, O. Cramariuc, T. Hukka, H. Lemmetyinen, T. T. Rantala, F. Dumitrascu*, "Optical spectroscopiccharacteristics and TD-DFT calculations of new pyrrolo(1,2-b)pyridazinederivates", J. Photochem. Photobiol. **A194**, 2008, pp 308-317.
[18].*S. Tumkevicius, J. Dodonova, K. Kazlauskas, V. Masevicius, L. Skardziute, S. Jursenas*, "Synthesis and photophysical properties of oligoarylenes with a pyrrolo[2,3-d]pyrimidine core", Tetrahedron Lett. **51**, 2010, pp 3902-3906.
[19].*L. Skardziute, K. Kazlauskas, J. Dodonova, J. Bucevicius, S. Tumkevicius, S. Jursenas*, "Optical Study of the Formation of Pyrrolo[2,3-d]pyrimidine-based Fluorescent Nanoaggregates", Tetrahedron, **69**, 2013, pp 9566-9572.
[20].*J. Bucevicius, L. Skardziute, J. Dodonova, K. Kazlauskas, G. Bagdziunas, S. Jursenas, S. Tumkevicius*, "2,4-Bis(4-aryl-1,2,3-triazol-1-yl)pyrrolo[2,3-d]pyrimidines: Synthesis and Tuning of Optical Properties by Polar Substituents", RSC Adv. **5**, 2015, pp 38610-38622.
[21].*S. Goswami, S. Chakraborty, S. Paul, S. Halder, A. C. Maity,* "A simple quinoxaline based highly sensitive colorimetric and ratiometric sensor, selective for nickel and effective in very high dilution", Tetrahedron Lett. **54**, 2013, pp 5075-5077.
[22].*Y. Zhang, Y. Yan, S. Chen, Z. Gao, H. Xu*, "Naked-eye' quinoline-based 'reactive' sensor for recognition of Hg^{2+} ion in aqueous solution", Bioorg. Med. Chem. Lett. **24**, 2014, pp 5373-5376.
[23].*R. El Aissi, J. Liu, S. Besse, D. Canitrot, O. Chavignon, J. M. Chezal, E. Miot-Noirault, E. Moreau*,"Synthesis and biological evaluation of new quinoxalinederivatives of ICF01012 as melanoma-targeting probes", ACS Med. Chem. Lett. **5**, 2014, pp 468-473.
[24].*J. Y. Li, C. Y. Chen, W. C. Ho, S. H. Chen, C. G. Wu,* "Unsymmetrical squaraines incorporating quinoline for near infrared responsive dye-sensitized solar cells", Org. Lett.**14**, 2012, pp 5420-5423.
[25].*W. Yingm J. Yang, M. Wielopolski, T. Moehl, J. E. Moser, P. Comte, , J. Hua, S. M. Zakeeruddin, H. Tian, M. Gratzel*, "New pyrido[3,4-b]pyrazine-based sensitizers for efficient and stable dye-sensitized solar cells", Chem. Sci. **5**, 2014, pp 206-214.
[26].*A. J. Huckaba, F. Giordano, L. E. McNamara, K. M. Dreux, N. I. Hammer, G. S. Tschumper, S. M. Zakeeruddin, M. Gratzel, M. K. Nazeeruddin, J. H. Delcamp*, "Indolizine based donors as organic sensitizer components for dye-sensitized solar cells", Adv. Energ. Mater. **5**, 2014, 1401629.
[27].*N. Srividya, P. Ramamurthy, V. T. Ramakrishnan*, "Photophysical studies of acridine(1,8)dione dyes: a new class of laser dyes", Spectrochim. Acta Mol. Biomol. Spectrosc. **54**, 1998, pp 245-253.
[28].*A. R. Katritzky, C. A. Ramsden, E. F. V. Scriven, R. J. K. Taylor*, Comprehensive Heterocyclic Chemistry III, Vol. **11**, Elsevier Science, Amsterdam, 2008.
[59].*E. Georgescu, F. Georgescu, M. M. Popa, C. Draghici, F. Dumitrascu, L. Tarko*, "Efficient one-pot, three-component synthesis of a library of pyrrolo[1,2-c]pyrimidine derivatives". ACS Comb. Sci., vol. **14**, 2012, pp. 101-107.
[60].*E. Georgescu, F. Georgescu, C. Draghici, L. Cristian, M. M. Popa, F. Dumitrascu*, "Fast and green one-pot multicomponent synthesis of a library of pyrrolo[1,2-*c*]pyrimidines under microwave irradiation" Combinatorial Chemistry & High Throughput Screening Discovery, vol. **16**, iss 10, 2013, pp. 851-857.
[348]. *H. Brederek, R. Gompper, B. Geiger*, "Synthese von Pyrimidinen mittels Tris-formamino-methans ", Chem. Ber., vol. **93**, 1960, pp. 1402-1406.
[349]. *M. M. Popa, E. Gerorgescu, M. R. Caira, F. Gerorgescu, C. Draghici, R. Stan, C. Deleanu, F. Dumitrascu,* "Indolizines and pyrrolo[1,2-c]pyrimidines decorated with a pyrimidine and a pyridine unit respectively", Beilstein J OrgChem., vol. **11**, 2015, pp. 1079-1088.

[350]. *M. L. Tatu, E. Georgescu, C. Boscornea, M.M. Popa, E.-M. Ungureanu*, Syntesis and fluorescence of new 3- biphenylpyrrolo[1,2-c]pirimidines, International symposium, Priorities of Chemistry for a Sustainable Development, PRIOCHEM, XI edition, Bucharest, Octomber 29 – 30, 2015.

[351]. *M. L. Tatu, E. Georgescu, C. Boscornea, M. M. Popa, E. M. Ungureanu*, Syntesis of new 3-phenylpyrrolo[1,2-c]pirimidines, International Symposium „Mediul și Industria (Enviroment and Industry)" – SIMI 2016, Octomber 13-14, Bucharest.

[352]. *M. Ziołek, K. Filipczak, A. Maciejewski*, "Spectroscopic and photophysical properties of salicylaldehyde azine (SAA) as a photochromic Schiff base suitable for heterogeneous studies", Chem. Phys. Lett., vol. **464**, 2008, pp. 181–186.

[353]. *M. S. Zakerhamidia, A. Ghanadzadeha, H. Tajalli, M. Moghadamb, M. Jassas, R. Hosseininiaa*, "Substituent and solvent effects on the photo-physical properties of some coumarin dyes", SpectrochimicaActa Part A, vol. **77**, 2010, pp. 337–34.

[354]. *N. Mataga, T. Kubota,* Molecular Interactions and Electronic Spectra, Marcel Dekker, New York, 1970, pp. 371–410.

[355]. *M. Ravi, T. Soujanya, A. Samanta, T. P. Radhakrishnan*, "Excited-state dipole moments of some Coumarin dyes from a solvatochromic method using the solvent polarity parameter, E^N_T", J. Chem. Soc. Faraday Trans., vol. **91**, 1995, pp. 2739–2742.

[356]. *A. Kawski*, "On the Estimation of Excited-State Dipole Moments from Solvatochromic Shifts of Absorption and Fluorescence Spectra Z", Naturforschung, vol. 57, 2002, pp. 255-262.

[357]. *R. Ghazy, S. A. Azim, M. Shaheen, F. El-Mekawey*, "Experimental studies on the determination of the dipole moments of some different laser dye", Spectrochim. Acta Part A, vol. **60**, 2004, pp. 187-191.

[358]. *M. J. Kamlet, R.W. Taft,* "The solvatochromic comparison method. I. The .beta.-scale of solvent hydrogen-bond acceptor (HBA) basicities", J. Am. Chem. Soc., vol. **98**, 1976, pp. 377-383.

[359]. *L. Liu, Y. Sun, S. Wei, X. Hu, Y. Zhao, J. Fan*, "Solvent effect on the absorption and fluorescence of ergone: Determination of ground and excited state dipole moments", Spectrochim. Acta Part A, vol. **86**, 2012, pp. 120-123.